PNNL-29774

Pacific Northwest
NATIONAL LABORATORY
Proudly Operated by Battelle Since 1965

PNNL-Recommended CISCC Measurement Test Plan for the NRC

Prepared for the U.S. Nuclear Regulatory Commission

February 2020

Mychailo B. Toloczko

U.S. DEPARTMENT OF
ENERGY

PNNL-29774

PNNL-Recommended ClSCC Measurement Test Plan for the NRC

Mychailo B. Toloczko

February 2020

Prepared for: U.S. Nuclear Regulatory Commission
NRC COR: Bruce Lin
NMSS Advisor: Darrell Dunn

PNNL operates under DOE contract DE-AC05-76RL01830

Pacific Northwest National Laboratory
Richland, Washington 99354

Abstract

This document presents a suggested approach to quantitative assessment of chloride-induced stress corrosion cracking (CISCC) behavior of dry cask storage system (DCSS) stainless steel canisters that are stored outside at nuclear power plants. A review of state-of-the-art in stress corrosion crack growth rate (SCCGR) measurement techniques developed in the light water reactor industry is provided and compared with the body of literature on CISCC measurements relevant to DCSSs where nearly all studies have used much more simplistic methods that provide reduced data precision or no growth rate data at all, generally resulting a large amount of uncertainty in crack growth rate estimates. A 4-point bend test specimen instrumented for in-situ measurement of crack length is recommended for use in CISCC growth rate studies over compact tension specimens that have traditionally been used for SCCGR measurements because a 4-point bend method allows for quantifiable, controlled deposition of salts on surfaces with short cracks. Finally, a suggested 4-6 year test plan is provided that will evaluate CISCC growth rate as a function of several important parameters such as temperature, salt concentration, salt type, stress intensity, material-to-material variability, and material deformation level.

Acknowledgments

The authors gratefully acknowledge discussions with Darrell Dunn of the U.S. Nuclear Regulatory Commission.

Contents

Figures

Acronyms

3PB	3-point bend
4PB	4-point bend
BWR	boiling water reactor
CGR	crack growth rate
CHR	crystallization relative humidity
CISCC	chloride-induced stress corrosion crack(ing)
CRDM	control rod drive mechanism
CT	compact tension
CW	cold work
DCPD	direct current potential drop
DCSS	dry cask storage system
DOE	US Department of Energy
DRH	deliquescent relative humidity
FEM	finite element model(ing)
GB	grain boundary
HAZ	heat effected zone
IGSCC	intergranular stress corrosion cracking
ISFSI	independent spent fuel storage installation
K	stress intensity
LWR	light water reactor
NASA	National Aeronautics and Space Administration
NRC	Nuclear Regulatory Commission
PNNL	Pacific Northwest National Laboratory
PWR	pressurized water reactor
PWSCC	pressurized water stress corrosion cracking
RH	relative humidity
SCC	stress corrosion crack(ing)
SCCGR	stress corrosion crack growth rate
SCCI	stress corrosion crack initiation
SFWD	Spend Fuel Waste Disposition (program)
SNL	Sandia National Laboratories
SRNL	Savannah River National Laboratory
TGSCC	transgranular stress corrosion cracking
TT	thermally treated
xLPR	Extremely Low Probability of Rupture (a cooperative NRC-EPRI program)
YS	yield stress

1.0 Introduction

Chloride induced stress corrosion cracking (CISCC) is a possible degradation mechanism for spent nuclear fuel (SNF) dry cask storage systems (DCSSs). DCSSs are currently the most common means for extended storage of SNF in the USA and in some other countries. Their usage in the USA began 34 years ago at the Surry Nuclear Power Plant in VA and were originally intended to be used as a short term (~20 year) solution while a permanent long term repository was created. Thus, long term storage in DCSS was not a prominent factor in their design (including materials selection) and construction. However, because of delays in establishing a disposition pathway for SNF, it has become necessary to store SNF in DCSSs for periods that are longer than were originally intended. The primary potential issue with their extended use is CISCC of the exterior of the cask. These containers are typically made from 304 stainless steel (SS) that is susceptible to CISCC under certain conditions, namely when the material is under a sufficiently high tensile stress and is subjected to a sufficient quantity of a chloride-containing salt along with a sufficiently humid environment in the absence of any inhibitors. The nuclear power plants (NPPs) where these containers are stored are located at a variety of different geographical locations, including near oceans, industrial environments, dusty environments, etc., where CISCC has a chance of occurring. CISCC of stainless steel industrial equipment is known to occur under the described environmental conditions, and thus there is a concern that DCSSs could also undergo CISCC.

In prior research at Southwest Research Institute that was funded by the NRC **[1]**, a large study was conducted to evaluate environmental conditions where CISCC of stainless steel can occur. The NRC now desires to measure CISCC behavior under a range of relevant environmental conditions including both bounding conditions and more realistic conditions. Efforts by the U.S. Department of Energy and Industry to characterize the material and environmental conditions of DSCCs at various locations is underway. While CISCC has been a known issue for many years in other industrial environments and has been an urgent concern for DCSSs in countries where CISCC is more likely, such as Japan, the techniques that have been used to-date to measure CISCC have been simplistic and/or not optimally executed compared to techniques used in other industrial applications where there is a strong, ongoing need to accurately and precisely assess SCC behavior. Presented here is a recommended test CISCC test plan based on the use of advanced SCC testing methods. Pacific Northwest National Laboratory (PNNL) has 15 years of experience performing state-of-the-art SCC testing of nickel-base alloy light water reactor (LWR) pressure boundary components. In-situ measurement of time to crack initiation and crack growth rate are routinely conducted in conjunction with active load control using specimens that produce easily determined stresses and/or stress intensities. The test plan presented here assumes similar capability would be available in a CISCC test system but envisions a unique test specimen geometry that is better suited to CISCC testing than the types of specimens that have been used for LWR SCC testing. A full description of this test specimen geometry and its development are presented in this document, and proof testing steps where the cracking behavior of this new test specimen geometry can be compared to the established LWR SCC test specimen geometry are included in the recommended test plan.

2.0 Review of SCC and SCC Testing Concepts

SCC is a multi-step process in the regard that it includes both initiation and crack growth (Figure 1). The initiation step is typically considered to be comprised of two or more smaller steps of which the details depend on the controlling mechanism. For LWR SCC, this could include elemental redistribution on grain boundaries (GBs), the formation of a leading oxidation front on GBs, and eventually the formation of short cracks. For CISCC, the steps to initiation for a stainless steel may include development of a local corrosion cell, pit formation and growth, and then crack nucleation off a pit. The definition of an initiated crack is dependent on perspective. In terms of physical presence, initiation can be the point at which an observable crack forms, however, the ability to resolve a crack is dependent on the examination technique. Cracks with an opening as narrow as 30 nm are resolvable by scanning electron microscopy under some conditions while resolution by optical methods is likely to require a crack opening >10 μm **[2-4]**. Rather than define initiation by some physical attribute of the crack (e.g., a minimum crack opening, length, or depth), PNNL denotes the point of initiation as the time at which nucleated cracks begin to grow more rapidly into a specimen. After a crack has formed to a certain depth, stable crack growth can be observed if the crack tip conditions are held steady and the microstructure of the material is uniform.

SCC initiation and growth are classified as phenomena that take place at constant stress or stress intensity, respectively. The addition of cyclically controlled loading or straining, or even monotonic load or strain changes over relatively long periods of time such as a few weeks can cause an accelerated response that is not classified as pure SCC. Thus, SCC measurements, whether it be initiation or growth, should be performed under constant stress or stress intensity conditions, respectively.

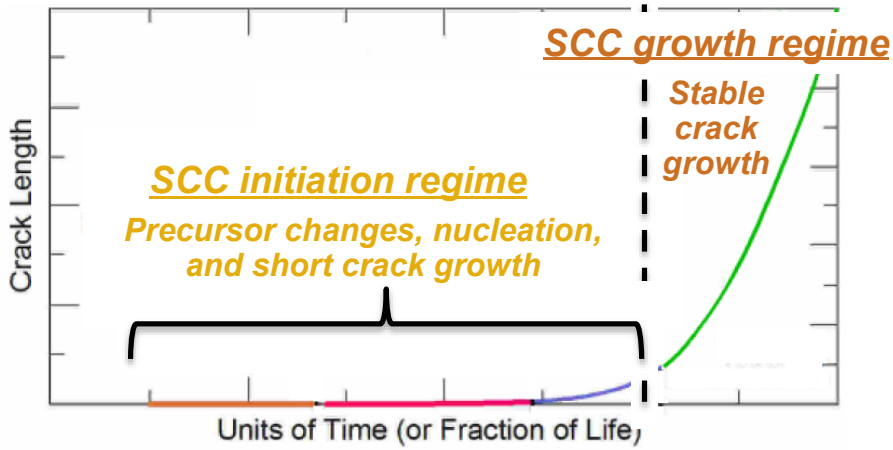

Figure 1. SCC as a multi-step process.

3.0 LWR Stress Corrosion Testing

3.1 Overview

In order to better understand the state of CISCC testing, it is beneficial to provide a review of the state of the art in stress corrosion testing of materials exposed to LWR cooling water. Due to the critical importance of understanding the time to through wall cracking of LWR pressure boundary components, SCC testing in support of the light water industry has evolved to an advanced state where accurate quantitative data on growth rates and time to initiation are now routinely obtained. PNNL is among a handful of laboratories across the world that have developed this capability, and so a review of the PNNL capability **[5-7]** is provided here as an example of the quantitative data that can potentially be attained for evaluation of CISCC.

An important center piece of LWR SCC testing is the ability to perform in-situ measurement of cracking response whether it be crack initiation or crack growth. All successful LWR SCC testing laboratories have accomplished this through the direct current potential drop (DCPD) technique whereby a precisely controlled constant current is run through a specimen, and the formation of a crack or a change in crack length is detected by measuring the change in voltage across the region of a specimen where a cracking is expected to occur. The formation of a crack or crack extension is detected as an increase in voltage across this region. This is a conceptually simple technique, but in practice it is difficult to accomplish because the formation of a crack or changes in crack length are typically represented as nanovolt level changes in potential that require a clear understanding of techniques to produce a useful signal-to-noise ratio (SNR) to see these changes.

Quantitative, in-situ LWR SCC growth rate (SCCGR) measurements are accomplished using compact tension specimens while in-situ crack initiation times are currently determined using tensile specimens. A sketch of the DCPD wiring arrangement configured for a single compact tension crack specimen is shown in Figure 2. As with all DCPD measurement systems, a constant current is run through a specimen, and the voltage across the crack plane is measured and converted into a crack length by means of an empirically derived formula relating voltage to crack length. The use of additional back face voltage measurement probes to provide reference-corrected data is an option that exists and is often needed in cases where significant resistivity evolution is expected to occur in the specimen material at the test temperature. SCC initiation is monitored using DCPD as well with the target voltage measurement points depicted in Figure 3. The voltage measurement across the gauge region is sensitive to the formation of cracks. As with SCCGR testing, a reference voltage measurement is needed for some combinations of material and test conditions where resistivity evolution of the material occurs. The requisite SNR is accomplished by a combination of best practice techniques to reject of electro-magnetic interference and precise control over environmental conditions.

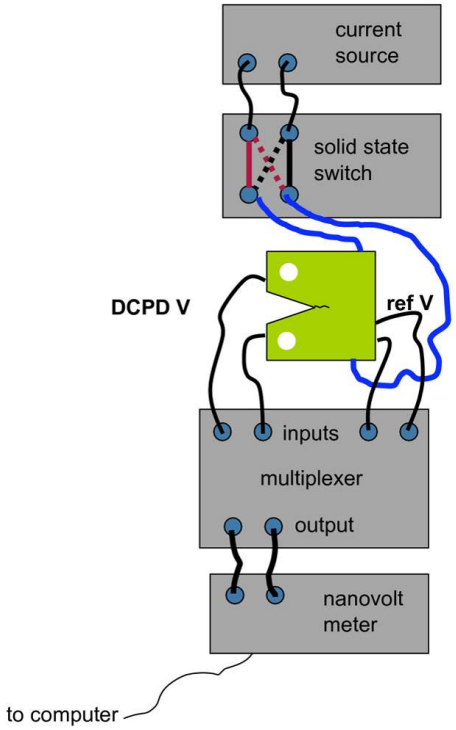

Figure 2. Schematic representation of DCPD data acquisition system and voltage probe locations as used in SCCGR testing of CT specimens.

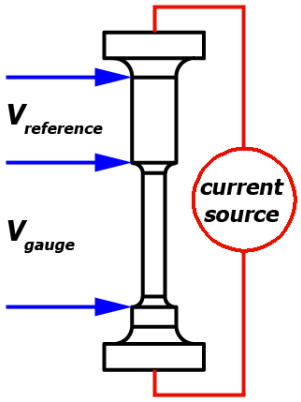

Figure 3. PNNL SCC initiation tensile specimen showing target DCPD measurement points.

These test systems have precise control over all aspects of environment. Key parameters that can readily be observed and recorded to assess environmental stability are autoclave temperature, applied load, and autoclave pressure. An example of these measurements taken over a period of ~3 days in a PNNL test system is provided in Figure 4. Temperature is extremely stable with a variation of +/- 0.1°C. Servo load is also very stable, exhibiting moment-by-moment load fluctuations of +/- 0.5 kg that are probably due more to noise in the electronics than to an actual variation in load. Tare load on the pullrod that is controlled by water pressure is also stable to within +/- 0.5 kg on a moment-by-moment basis, but due to variation in high-pressure pump performance, there is a day-by-day variability of +/- 1.5 kg. This results in a total load variability of +/- 2 kg and represents a <0.5% variability applied load for the typical target test load of ~1360 kg.

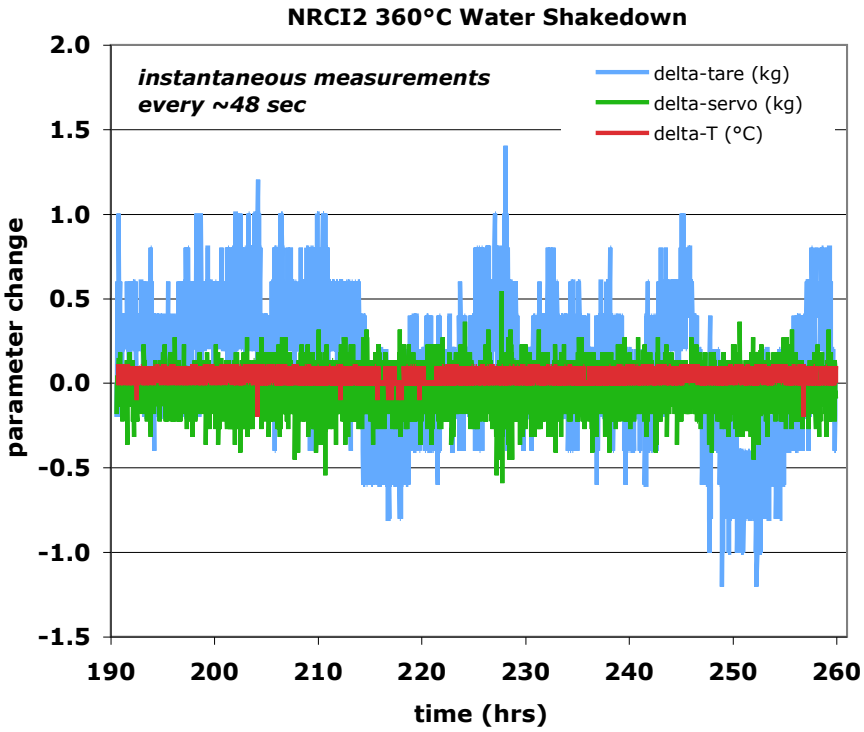

Figure 4. Variation in servo load, tare load, and autoclave temperature as a function of time for the NRCI2 test system.

Consistency of temperature throughout the autoclave is an important trait needed for good test results. Temperature in these test systems is measured in the autoclaves at several different locations using an array of four adjustable thermocouple probes, and in PNNL's largest test systems, a 2°C maximum spatial variation was observed during testing at 360°C. The coldest location was at the bottom of the load train, while the warmest was about 2/3 of the way up the load train.

Other aspects of the environment such as mixing loop temperature, autoclave water conductivity, autoclave pressure, dissolved gas content, mixing loop water chemistry, and autoclave pressure are all controlled and measured either directly or indirectly.

The high degree of environmental stability allows the PNNL DCPD system to provide high resolution measurement of crack growth rate or crack initiation time. The DCPD noise levels are sufficiently low to measure crack growth rates as low as 1×10^{-9} mm/s (~30 µm/year) in high temperature water. An example of a SCCGR test on a moderately SCC resistant material is provided in Figure 5, and the first SCC observation is shown in greater detail in Figure 6. DCPD noise levels are no greater than ±1 µm, allowing for low crack growth rates (CGRs) to be determined in a relatively short period of time.

PNNL test systems are capable of maintaining a constant stress intensity on SCCGR test specimens. This is accomplished through the custom software that has full control over servo load and continually reads the DCPD voltages. The voltages are converted to a crack length, and then servo load is adjusted to maintain a target stress intensity.

For SCCGR tests, the ability to perform in-situ measurement of crack length allows for observing the effect of controlled variation of test environment on-the-fly on a particular specimen or on multiple specimens simultaneously. The effect of a systematic variation in stress intensity, temperature, and water chemistry are all routinely assessed, such as shown in Figure 5 where the effect of stress intensity on SCCGR susceptibility was evaluated as the test progressed.

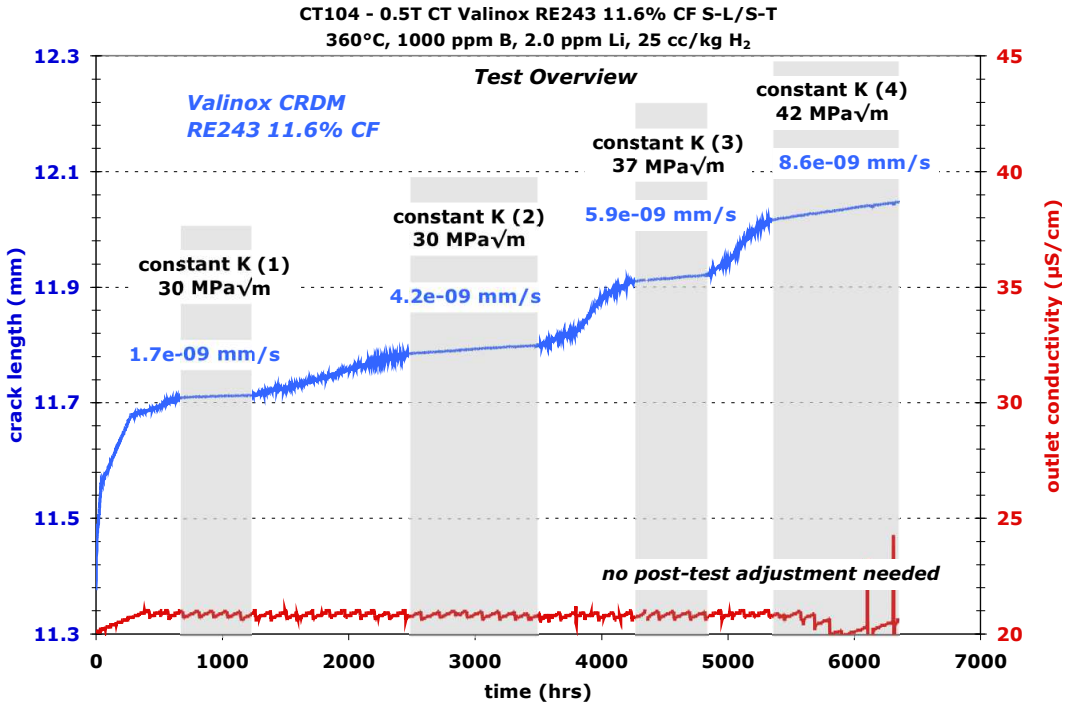

Figure 5. SCCGR test of a 12% cold forged, thermally treated (TT) Alloy 690 material that exhibited low-to-moderate SCC growth resistance.

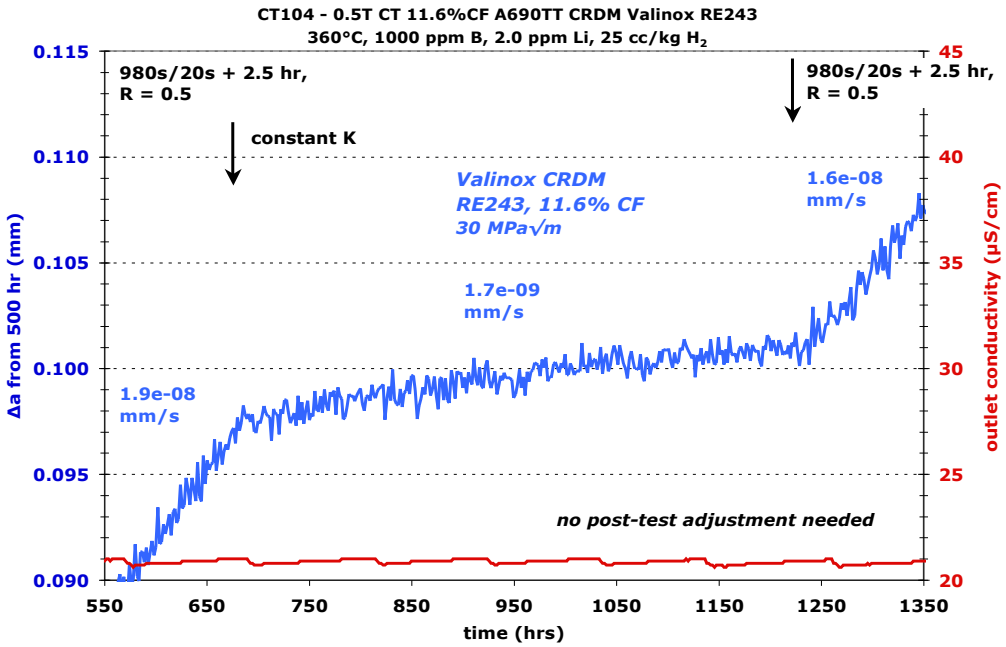

Figure 6. First SCC observation during an SCCGR test of a 12% cold forged Alloy 690TT material that exhibited low-to-moderate SCC growth resistance.

Another important evolution in SCC test methods for LWR cooling water environments is the ability to perform multi-specimen tests while obtaining quantitative SCC data. PNNL has developed the capability to test up to six SCCGR specimens simultaneously and up to 36 SCC initiation specimens simultaneously. An example of one of our small test systems is provided in Figure 7. As is indicated in the figure, specimens are serially loaded except for SCC initiation tests of more than 12 specimens where a combination of serial and parallel loading are used. In either scenario, all specimens experience the same applied load.

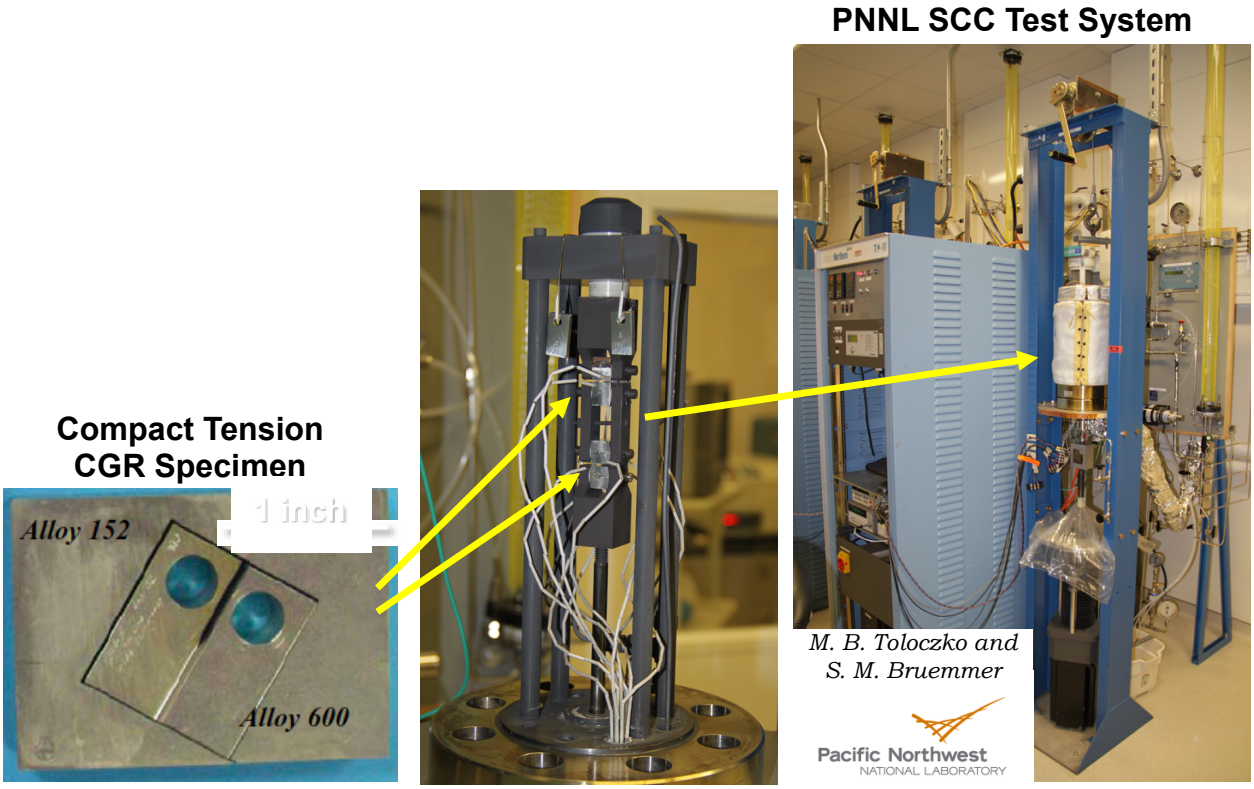

Figure 7. PNNL small autoclave test system containing two compact tension crack growth rate measurement specimens.

3.2 SCC Crack Growth Rate Testing Details

An important aspect of SCCGR testing is management of specimen response during a test. SCC in some materials occurs much more rapidly on grain boundaries than through the matrix. For those materials, it is important to make sure that the crack has an opportunity to find grain boundaries. SCCGR tests always are started from a machined notch such as shown for a CT specimen in Figure 8. The first step for an SCC test is nucleating and growing a fatigue precrack from the machined notch. For single specimen test systems, this step can be performed in the stress corrosion test environment. Since there can be a fair amount of variability in the time it takes to nucleate the precrack, specimens for a multispecimen test must be precracked individually. This can be done in a stress corrrosion environment as well, but many labs that perform multispecimen tests will fatigue precrack in air at room temperature. Air fatigue precracking has no adverse effect on an SCC test because the precrack is always extended further in the environment before attempting obtain SCC data. Then through a series of more and more

gentle cyclic loading transitioning steps that are typically concluded with a constant stress intensity observation, the fatigue precrack is given the chance to evolve into a stress corrosion crack. This sequence is typically called "transitioning". The reasons why transitioning is needed can vary with the material being tested. In general, the crack tip shape needs to be evolved from a comparatively blunt fatigue crack to a sharp crack that would be characteristic of a growing SCC crack. In materials where intergranular stress corrosion cracking (IGSCC) is the dominant mechanism, then the fatigue crack must be given the chance to intersect grain boundaries under favorable SCC conditions. The likelihood of the fatigue crack staying on the grain boundary will depend on a combination of the aggressiveness of the fatigue cycling rate and the susceptibility of the grain boundaries.

In materials that are highly susceptible to IGSCC, little or no transitioning is needed beyond producing a fatigue precrack because as the fatigue crack encounters grain boundaries, the crack will have a strong desire to stay on the boundaries despite rapid fatigue loading conditions that try to force the crack straight ahead irrespective of the local microstructure. However, for resistant materials, substantial transitioning steps are often needed to give the crack a chance to transition to SCC behavior. This generally involves applying more and more gentle cyclic loading steps, with the exact conditions at each step dependent on the material and susceptibility. One example is provided in Figure 5 where two attempts to measure SCCGR in LWR cooling water conditions at 30 MPa√m were performed, and the second observation exhibited a higher rate. The higher rate for the second measurement suggests that transitioning was more favorable the second time and that a greater fraction of the crack front was undergoing IGSCC. For substantially resistant materials, such as in Figure 9, multiple transitioning attempts may not yield a higher SCCGR. For materials that exhibit transgranular stress corrosion cracking (TGSCC), such as some stainless steels under some environmental conditions, the goal of the transitioning sequence is to produce a sharp crack that has the best chance of exhibiting stable growth at constant stress intensity.

Another aspect of specimen management is controlling the degree of SCC behavior along the length of the crack. SCC behavior can vary across the crack front due to many factors such as local chemistry, internal stress, and degree of local strain. In some cases, the crack front can become uneven or become held back in some portions. This is especially prevalent for intergranular SCC in weld metals. It is important to periodically take steps to straighten the crack front and/or assess the degree of unevenness. Typically, this involves enabling cyclic loading to move the crack forward by corrosion fatigue or pure fatigue growth that is less susceptible to local variations in factors that affect SCC susceptibility. The strength of the load cycling that is applied depends on the degree of straightening that is thought to be needed. Once the crack is thought to have been straightened, loading conditions are transitioned back to constant stress intensity SCC conditions.

For multi-specimen SCCGR tests, it is important to select materials that are expected to have roughly similar crack growth response. Crack tip stress intensity, K, is a function of both load and crack length, and since all specimens experience the same load, any substantial divergence in crack length among the specimens over the course of a test will cause a divergence in K. In cases where CGR exhibits a K dependence, the divergence in K follows a positive feedback loop whereby specimens that exhibit faster crack growth will experience an increasingly higher K. For small differences in crack length, divergence is minimal. The most common way to make good use of a multi-specimen test is to evaluate several duplicate specimens and/or multiple heats of the same material to build up confidence in the observed SCC response. PNNL typically tests at least two specimens for every unique condition of material and environment being studied in the LWR SCC testing programs.

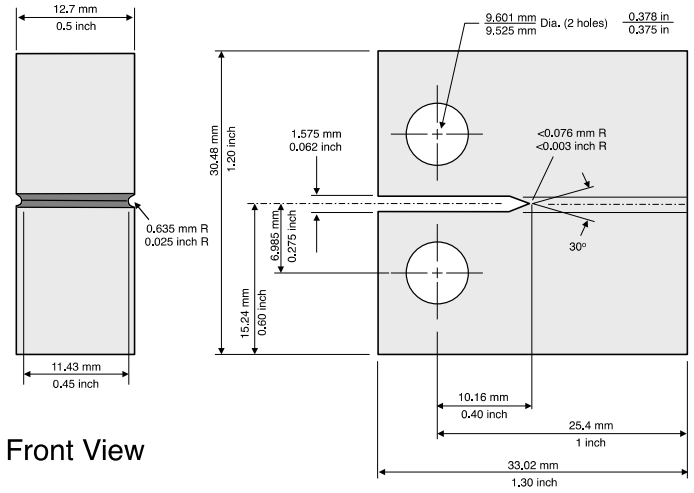

Figure 8. "Half size" (0.5T) compact tension specimen used for SCCGR testing at PNNL.

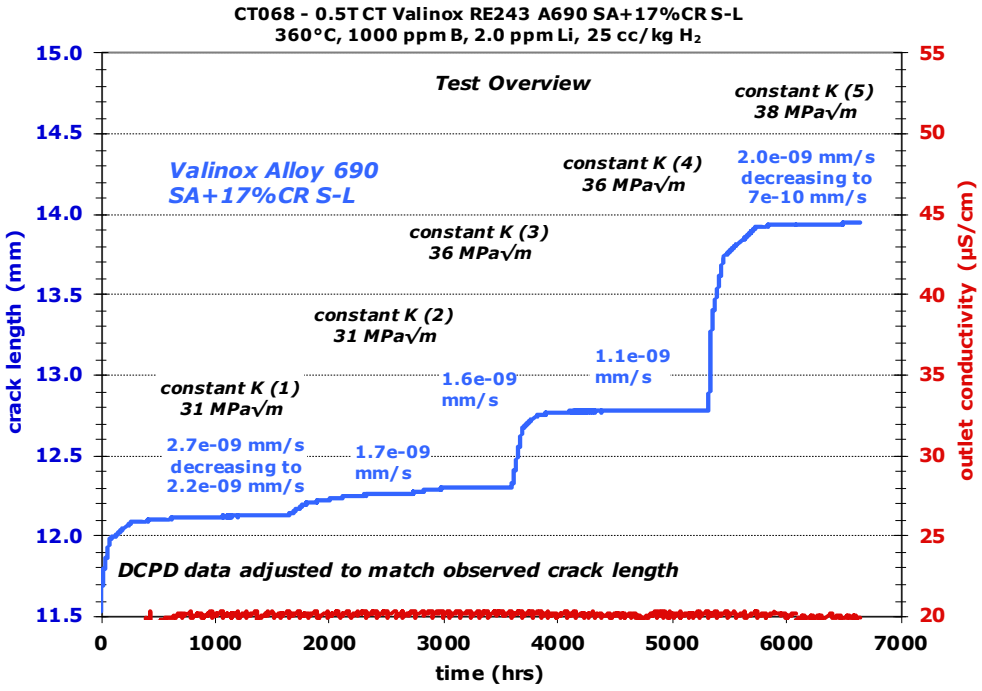

Figure 9. SCCGR test of a 17% cold forged, solution annealed Alloy 690 material that exhibited substantial SCC growth resistance.

3.3 SCC Initiation Testing Details

As already mentioned, PNNL uses unnotched tensile specimens held at constant load for stress corrosion crack (SCCI) testing. An unnotched tensile specimen allows initiation to occur anywhere along the full gauge length, thus sampling a greater amount of microstructure compared to a notched specimen. Crack initiation is monitored in-situ by DCPD, and cracks are detectable at a depth of 100-150 µm, well

before they can be detected by optical methods. This combination of in-situ measurement and high sensitivity to crack formation allows for more accurate measurement of initiation time.

The general testing methodology is much different than for SCCGR testing. For an SCCGR test, the crack must be given a chance to find the most susceptible microstructures, whereas for an SCCI test, all available microstructures from which a crack can initiate are already present (the surface of the specimen). Thus, no active promotion of the initiation process needs to be performed except to maintain a stable environment.

This difference in testing approach also extends to confirming material behavior. For an SCCGR test where crack length is measured in-situ, multiple microstructures can be assessed by driving the crack forward to new regions. An equivalent approach is not possible for an SCCI testing, and any variability in material behavior, i.e., variability in microstructure, is assessed through testing multiple specimens.

Selection of an appropriate test load is simplified compared to an SCCGR test. The target stress intensity for an SCCGR test can depend on a number of factors such as material strength, expected in-service stress intensity values, and a need to be at a stress intensity that is sufficiently beyond the threshold stress for SCC growth. Two realms of loading are possible SCC initiation testing – these are testing at the yield stress (YS) and testing below the YS. It is important to recognize that it's not possible to test a material above its YS. If the stress is driven beyond the YS, then the material is fundamentally altered (deformation added), and the response is not representative of the original material. For LWR SCCI testing, loading specimens to their YS is generally considered to be the baseline test condition. This is because it is acknowledged that reactor pressure boundary components can have some amount of deformation due to a variety of reasons that will be discussed in Section 6, and therefore the surface structures can be loaded to their YS. The fact that such structures can be deformed means that laboratory test specimens may need to have applied cold work or be strained in-situ to reach equivalent expected deformation levels. Dry cask storage system (DCSS) containers will also have applied deformation by a variety of methods, and therefore, the baseline stress for CISCC testing should be the YS, probably with the material having some degree of cold work.

The traditional method for setting a tensile specimen to its test load has been to characterize the stress versus strain response of the material in advance through multiple tensile tests, identify the applied load associated with the desired fraction of the YS (including up to the YS), and then apply the associated target load to the specimen(s). Because of variability in homogeneity of a piece of material, there is always some regional variation in YS of the piece of material, and as a result, actual YS from specimen-to-specimen varies slightly, and actual YS fraction of a test specimen may be slightly above or below the target YS fraction of the specimen. Because of this, PNNL has developed a high-resolution technique for determining the actual YS fraction. The DCPD technique applied to tensile specimens is sensitive not only to crack formation, but also elastic and plastic deformation. If the DCPD noise levels are sufficiently low, it is possible to measure and record the stress versus strain response during specimen loading. This tracking of stress versus strain response can even be performed for multiple serially loaded specimens. In an example of a loading run of three Alloy 182 specimens shown in Figure 10 for an LWR SCCI test, one specimen began yielding earlier than the other two. In this case, load was increased until all specimens had reached at least 0.2% plastic strain (the standard condition for YS measurement). The ability to monitor the specimen during loading will reveal any abnormal specimen response, and it provides additional information for understanding SCCI response.

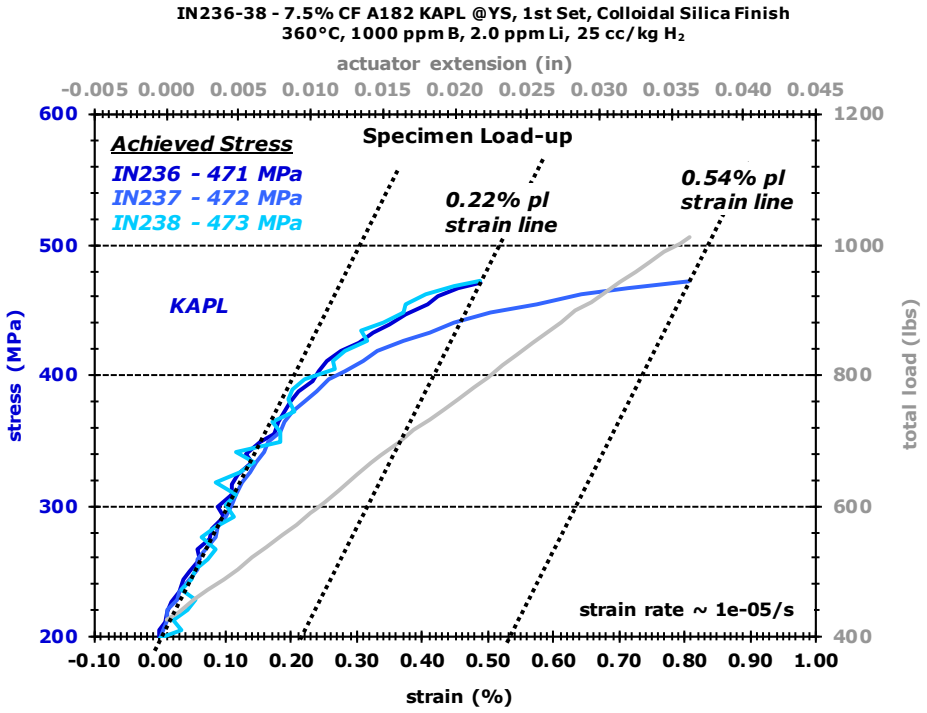

Figure 10. Stress versus strain plot obtained during loading of three Alloy 182 specimens to their yield stress for an SCCI test.

An example of a six-specimen SCC initiation test is provided in Figure 11. The data are plotted as strain because creep strain dominated the DCPD response up to the time of initiation. The initiation time as determined by in-situ continuous DCPD measurement is defined by the point where a curve exhibits a strong positive rate of change of curvature as marked by five of the six arrows in the plot. Physically, this change represents the point in time in which rapid crack growth begins. The crack growth rate in Ni-base alloys in LWR environments exhibit a threshold-like response where SCCGRs rapidly increase starting at ~10 MPa√m **[8]**. Post-test measurement of cracks in our initiated specimens have shown the crack depth to produce a stress intensity that corresponds to this threshold value **[6, 9]**. PNNL uses fixturing that allows a specimen to fracture in-situ without having to stop the test, however it is preferred to remove the specimen at the time of initiation (or shortly after) to allow characterization of the crack morphology at the onset of initiation.

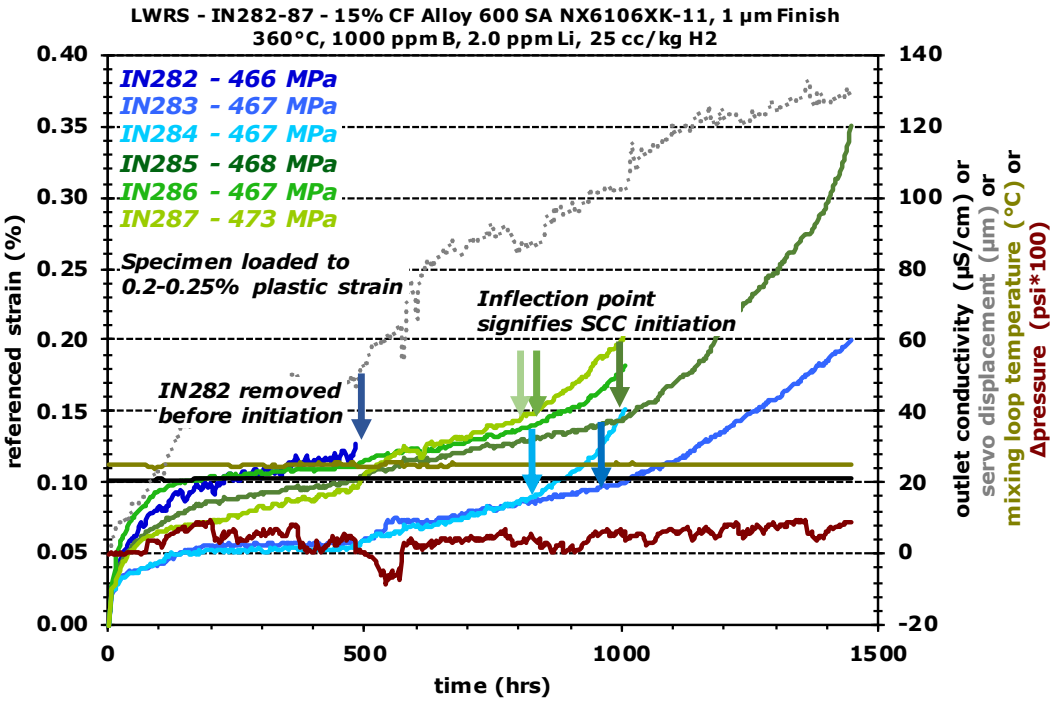

Figure 11. LWR SCC initiation response of six Alloy 600 specimens tested together in one system.

4.0 Review of Existing DCSS-Relevant CISCC Data

4.1 Overview

CISCC testing dates back many years due to the relevance of this degradation mode to metallic components near marine environments and some industrial environments. However, the majority of the data and information presented in this section was obtained from studies in support of DCSS systems. The data in the literature can provide insight on several aspects on the need for additional data, the development of a test methodology, and the creation of a baseline test plan. Aspects of the literature that are reviewed here include:

- CISCC behavior being observed. Was the test designed to observe crack initiation, crack growth rate, or general cracking response?
- Qualitative or quantitative observation. Was time to initiation and/or crack growth rate measured?
- Test specimen type and loading method. Was there passive or active control of stress and/or stress intensity? Is there knowledge of the stress and/or stress intensity values?
- Environments that have been used. Aqueous or humid air, salt type, salt concentration, salt replenishment.
- Crack initiation or crack growth rate values that have been reported or can be measured from the literature.

4.2 CISCC Behavior Being Observed

Methods for assessing CISCC response can be grouped into these basic types of observation:

- Crack/no crack observations.
- Time to crack initiation
- Average crack growth rate
- Time to failure
- Online crack growth rate measurement (live data)

Crack/no crack observations are typically used to evaluate relative CISCC susceptibility in different environments. Such tests, as for example by Albores-Silva **[10]**, Prosek **[11]**, and Fairweather **[12]**, will consist of a single exposure interval where the presence or number of cracks in specimens exposed to several different environments are compared. Because there is a single exposure interval, there is substantial uncertainty in any estimation of a crack initiation time. There is also the potential to estimate crack growth rate from such tests by sectioning the specimen to observe the crack depth. This type of CGR measurement may have large uncertainty due to a portion of the exposure period belonging to crack initiation time rather than crack growth.

Measuring time to crack initiation for CISCC studies has been achieved through periodic inspection of specimens such as by Shoji **[13]** and Kosaki **[14]**. The accuracy of the time to initiation depends greatly on whether the inspection intervals were appropriately spaced for the behavior of the specimens

An example of average crack growth rate can be found in the work of Duncan **[15]**, Hayashibara **[16]**, and Speidel **[17]**. In this type of test, the CGR is determined either by dividing a crack length increase by the total exposure time or by dividing the crack length by the total test time that includes both the time to

initiation and the time for crack growth. This latter methodology can result in significant underprediction of the actual crack growth rate.

Time to failure is affected by crack initiation time and crack growth rate. An example of this can be seen in the work of Tani **[18]**. If there are no mid test observations, then any estimates of crack initiation time are very approximate, and the measured average crack growth rate is under predicted.

Online crack growth rate measurement consists of a test where the specimen is instrumented to allow crack growth rate to be measured during the test. The most common method for this is the DCPD method that was described in Section 3 of this report. The only available DCSS related CISCC test effort utilizing DCPD that has been performed to-date was by Shirai at CREIPI **[19]**. This is a Japanese language report, although some portions of the results have been published in journals. Xie performed DCPD-based CISCC crack growth measurements for her Ph.D. research **[20]**, but to-date, the results have not been published in a journal. Turnbull has conducted DCPD-based CISCC crack growth rate measurements with a high degree of crack growth rate precision, but only in very dilute solutions of NaCl **[21]**.

4.3 Test Specimen Type and Loading Method

A wide range of specimens and loading methods have been employed such as U-bend **[22]**, C-ring **[23]**, tensile **[16]**, bend bar **[14]**, and compact tension **[15]**. Only properly designed 4-point bend and compact tension specimens are suitable for accurate, quantitative crack growth rate measurements. The other specimen types suffer from a lack of ability to control or even know stress intensity, so even if an average CGR is measured by destructive examination, it can be difficult to relate the observed cracking response to the environment because of a lack of knowledge of stress intensity. For light water reactor core water environments, Andresen **[24]** has shown that poor control over stress intensity, in particular, rapidly rising or falling stress intensity can cause much higher or much lower crack propagation rates than at a relatively steady stress intensity. It is not unreasonable to assume that such an effect may also exist for CISCC environments.

4.4 Test Environments

Constant relative humidity chambers (RH chambers) are readily available making it possible to produce deliquescent salts on specimens. However, there can be difficulty in applying known salt loadings to a specimen for a CISCC test. A common method is to apply droplets of a salt solution, allow the water to evaporate, and then place the specimen in the RH chamber **[11]**. This simple water evaporation method does not produce a uniform salt distribution on the specimen. There is also an emerging concern that over time, Cl may evaporate from deliquescent solutions, and thereby diminish or stop the CISCC reaction **[25]**. This suggests the possibility that continuous salt deposition such as that done by He and Mintz **[1, 26]** may be needed to accurately assess deliquescent salt CISCC effects. Another challenge for deliquescent salt CISCC tests is providing an opportunity for the deliquescent salt to move down a crack. The ability to know the salt concentration while allowing it to wick down a crack can most readily be accomplished by using a specimen where a crack grows from a smooth surface where the salt can be applied. This immediately eliminates compact tension specimens as an ideal means for measuring deliquescent salt CISCC behavior. This desire to have a surface where salt can readily be applied is the likely reason why nearly all deliquescent salt CISCC studies have been performed on either U-bend, C-ring, tensile, or bend bar specimens.

4.5 CISCC Measurements

The majority of the available CISCC growth rate measurements have been reported by Bryan **[27]** or Gorman **[28]**. CISCC may be dependent on a wide range of environmental parameters, but when viewed in aggregate as a function of temperature, both data compilations show an activation energy dependence of ~85 kJ/mol, albeit with a 100x scatter band across the entire temperature range **[29]**. Most certainly, some of this scatter is due to variations in environmental conditions being lumped together, but there is also a strong effect of the rudimentary crack length measurement methods that were employed. It is important to recognize that any bounding estimate of CISCC CGR will have to sit near the top of this uncertainty band, and any substantial improvement in the ability to accurately measure CGR can appreciably drop the bounding CGR estimate.

4.6 Literature Data Discussion

These examples are fully representative of the entire body of DCSS-relevant CISCC test data. While many of these tests provide information about the relative susceptibility of materials in different environments, very few of the published studies are capable of providing sufficiently accurate and reassuring CISCC growth rate measurements. This is partially a result of the simplicity of many of the tests that were never intended for measurement of crack growth rate. There are also some studies that reported unexpected results such as the work of CRIEPI where DCPD-measured crack growth rates slowed substantially after about 1 mm of crack propagation. Another example would be the stress intensity dependence. The work of Kosaki **[14]** and Tani **[30]** suggest a threshold stress intensity below 5 MPa√m for atmospheric CISCC for 316 SS while the work of Speidel in nearly saturated aqueous NaCl environments show a threshold above 20 MPa√m. These are two very different environments, but further assessment is clearly needed, especially since a low threshold stress intensity could have a large impact on predictions of CISCC.

5.0 CISCC Testing Needs and PNNL Approach

5.1 Crack Growth Rate Versus Initiation Time Measurement

There is a need to generate high precision, quantitative data to effectively evaluate CISCC susceptibility of DCSS **[27]**. For LWR pressure boundary components, the NRC has relied on crack growth rates much more strongly than SCC initiation times for setting inspection frequency over the last 30+ years because early service experience was fraught with a high incidence of cracking of the susceptible materials (Alloy 600 and Alloy 182) **[31, 32]**, and so there was no basis for using SCC initiation time. In recent years, the NRC and the LWR industry have been discussing and working towards using *SCC initiation times* (i.e., via Extremely Low Probability of Rupture (xLPR)) as an additional input for setting inspection frequency for LWR pressure boundary components **[33]**.

As with LWR pressure boundary components, it is likely that CISCC growth rates will be important for assessing container inspection intervals, and perhaps later, CISCC initiation times may be incorporated. Therefore, this test plan proposes to focus first on producing CISCC growth rate data, and then CISCC initiation time tests can be added to the test matrix later if needed.

5.2 Environment

PNNL will start first with aqueous tests. In comparison to humid air testing, a brine environment allows for a better estimate of water chemistry in the crack because there is an unlimited source of uniform concentration of solution to continually feed the crack. This will result in a more stable crack tip chemistry that is more strongly linked to the brine water bath. In comparison, for humid air testing, the degree of salt and water that migrate into the crack will not be known during a test, and post-test measurement of the solution chemistry after the test may not provide accurate information on the chemistry during the test. Because of the more consistent crack tip chemistry for aqueous tests, they can be thought of as bounding response or reference response tests. Data obtained from these tests will have substantial value in interpreting humid air tests where migration of a deliquescent solution to the crack tip is likely to be challenging and the change with time or position along the width of the crack. The intent will be to assess all relevant crack growth rate environmental dependencies in water, specifically temperature, stress intensity, salt composition, and salt concentration. This system will also be capable of assessing the effect of dissolved oxygen content, if desired. Material condition effects such as cold work level and heat-to-heat variability will also be assessed with relevance to known or expected canister material conditions. This will be discussed further in Section 6.

Another valuable aspect of testing in water is the ability to conduct on-the-fly changes in water chemistry because it allows for rapid evaluation of different salt concentrations including the addition of possible inhibitor compounds that may be present in DCSS environments. In contrast, for humid air testing any change in salt loading or chemistry must be performed as a separate test.

5.3 Selection of Test Method

CISCC tests conducted in air require applying a salt to the surface of the specimen in the region of cracking either before and/or during testing. In order to relate observed susceptibility to the environmental conditions, the amount of salt applied to the surface of the specimen in the vicinity of the crack must be controllable, uniform, and measurable. An exposed, easily observed surface in the vicinity of the crack greatly facilitates this. In comparison, it would be a challenge to apply salts and measure their concentration in the deep notch of a CT specimen (Figure 8) that is traditionally used for in-situ, quantitative CGR testing.

A rectangular bend bar specimen is an ideal geometry and has been used in some previous CISCC studies by others **[14, 19, 34]**, either in 2-point bend, a 3-point bend (3PB) or 4PB loading configuration. As part of another ongoing NRC project, PNNL has developed a 4PB test method for quantitative LWR SCC CGR and initiation time measurement. The 4PB test method was selected because this is intended to be a dual-use specimen for CGR testing and crack initiation testing, and for crack initiation testing, the outer tensile loaded surface of the specimen must have a relatively uniform stress over a useful length (at least 5 mm). A 3PB geometry produces a fairly concentrated stress directly under the center loading pin, but as will be shown, a 4PB geometry readily provides a region of uniform stress. The specimen can either have a notch for traditional CGR tests such as shown in Figure 12, or it can be machined to have a smaller width (W) value (6-10 mm) to be used for SCC initiation or shallow crack growth testing (Figure 13). The specimen can optionally have side grooves, and for this situation, the thickness value across the side grooves (B_{net}) remains at 9 mm while B elsewhere increases to ~11 mm.

5.4 4-Point Bend Specimen Development

The specimen size selected by PNNL was based on a number of requirements. First is that B had to be large enough to produce sufficient material constraint in the region of cracking for CGR testing. Morton has shown that crack bifurcation and/or atypical crack surface morphologies can occur if the specimen size to K ratio becomes too small **[35].** The formulation suggested by Morton is that $K \leq \sigma_{ys}\sqrt{(2B_{eff})}$. For testing of as received stainless steel that has a typical YS of ~220 MPa, a B value of 9 mm on a non-side grooved specimen allows for stress intensities up to 30 MPa$\sqrt{m}$. An 11 mm thick specimen with 8% depth side grooves gives a B_{eff} of ~10.6 mm provides an upper limit stress intensity of ~32 MPa$\sqrt{m}$. While side grooves are not required for CGR testing, they are generally preferable because they produce a more uniform stress intensity along the crack front, particularly near the sides of the specimen. Target applied load was also a factor in selecting specimen size. To accommodate the load carrying capability of the PNNL test systems, a target maximum specimen load of ~2000 lbs was established. Along with this there was a requirement to be able to test notched specimens with a starting ratio of crack length to section width (a/W) (Figure 12) of 0.2 and also be able to test unnotched specimens with shallow cracks having a depth of as little as 0.5 mm. These requirements worked together to set the specimen bending moment (and consequently a length of 62 mm) along with a W of 16 mm for notched specimen tests and an allowable W of ~10 mm for shallow crack tests.

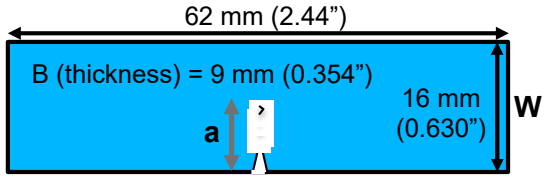

Figure 12. 4PB crack growth rate specimen.

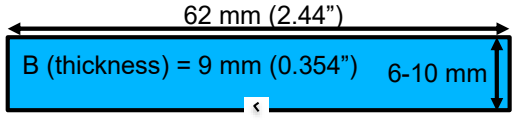

Figure 13. 4PB crack initiation and shallow crack growth specimen.

Extensive finite element modelling was performed to guide specimen design, obtain the stress intensity factor, and the crack length versus DCPD calibration. An example of the von Mises stress distribution of an uncracked specimen for the selected 4PB geometry is presented in Figure 14. A general feature of 4PB loading is that the stress on the tensile loaded surface is approximately uniform for the distance between the two inner load pads. An 11 mm spacing was selected, thus producing ~10 mm of uniformly loaded surface area to study crack initiation behavior.

Examples of von Mises stress fields produced in notched and shallow crack specimens are presented in Figure 15 and Figure 16, respectively for an elastic plastic material. The von Mises stress distribution that is representative of the plastic zone shape shows a typical Mode 1 appearance.

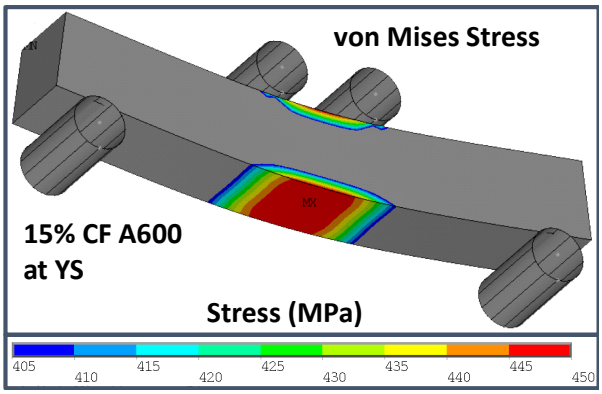

Figure 14. von Mises stress distribution as predicted for a 15% CF Alloy 600 4PB specimens loaded to its yield stress.

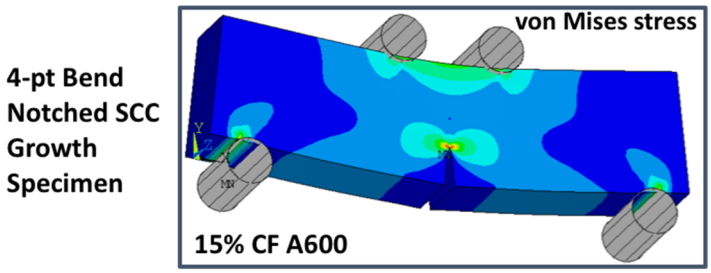

Figure 15. von Mises stress distribution for a notched 4PB specimen with an applied load and with an elastic-plastic constitutive response of a 15% cold-forged Alloy 600 material.

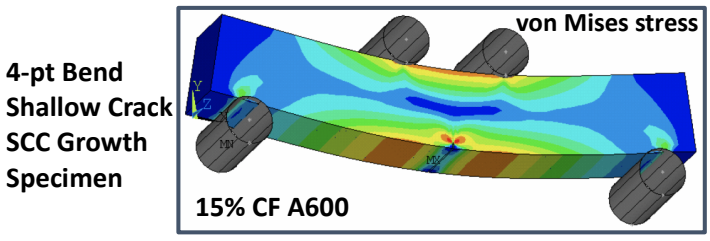

Figure 16. von Mises stress distribution for a shallow crack 4PB specimen with an applied load and with an elastic-plastic constitutive response of a 15% cold-forged Alloy 600 material.

While the 3PB stress intensity factor as a function of a/W is readily available from a multitude of sources, it was found that 4PB stress intensity was not readily available. The only citable derivation that could be found was one by the National Aeronautics and Space Administration (NASA) in 1965 **[36]** that covered a relatively narrow range of a/W, in particular, the lowest a/W was for their derivation was 0.1 whereas a stress intensity factor for a/W down to 0.02 was desired. Thus, finite element modeling (FEM) was used at PNNL to determine the relationship between normalized stress intensity and normalized crack length (Figure 17). As is typical for stress intensity derivations, linear elastic constitutive response was used in the model. The plot shows excellent agreement between the PNNL FEM-based result and the NASA analytic-based result lending confidence in the PNNL result.

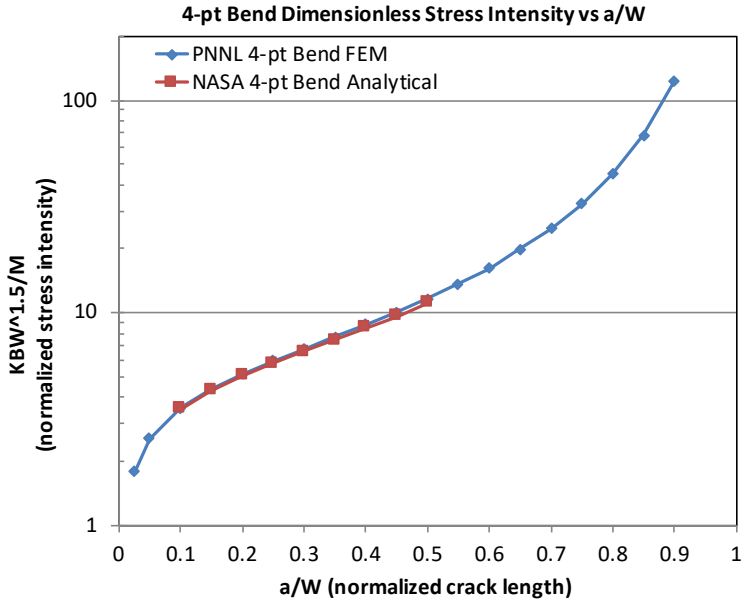

Figure 17. Normalized stress intensity versus normalized crack length. Plot shows PNNL result compared to a result produced by NASA in 1965 [36].

FEM was also used to determine the relationship between crack length and crack voltage using representative material resistivity values. Following the same methodology that is used for CT specimens, the crack voltage probes were targeted to be 1 mm from the bottom of the specimen and 1 mm away from the centerline of the specimen (Figure 18). While accurate placement of these probes is not critical for tracking the length of long cracks, it is very important for accurate estimation of the length of shallow cracks. Positioning the probes closer to the bottom of the specimen would improve signal sensitivity to change in length of shallow cracks, but 1 mm is a reasonably practical limit on how close a 0.5 mm thick wire can be spot welded near the edge of the specimen. Figure 18 also shows placement of reference DCPD voltage probes. These are needed when a material is expected to undergo resistivity evolution during testing. This happens for some Ni-base alloys being tested at LWR relevant temperatures, but there will be no resistivity change of any consequence for stainless steels being tested at DCSS CISCC-relevant temperatures, and thus reference probes unneeded. Normalized crack voltage plotted versus normalized crack length in Figure 19 reveals indeed DCPD sensitivity to crack length is low for shallow cracks. The slope and therefore the sensitivity substantially increase as a/W exceeds 0.1 which corresponds roughly to a 1 mm crack depth.

Curve fits to the stress intensity and the DCPD calibration have been incorporated into custom written software that was developed to run the CT specimen crack growth test systems. The crack growth software estimates crack length from DCPD and uses this to actively control stress intensity as cracking progresses. Either steady, increasing, or decreasing stress intensity versus crack length scenarios are possible, although the standard approach for SCC testing is to maintain constant stress intensity.

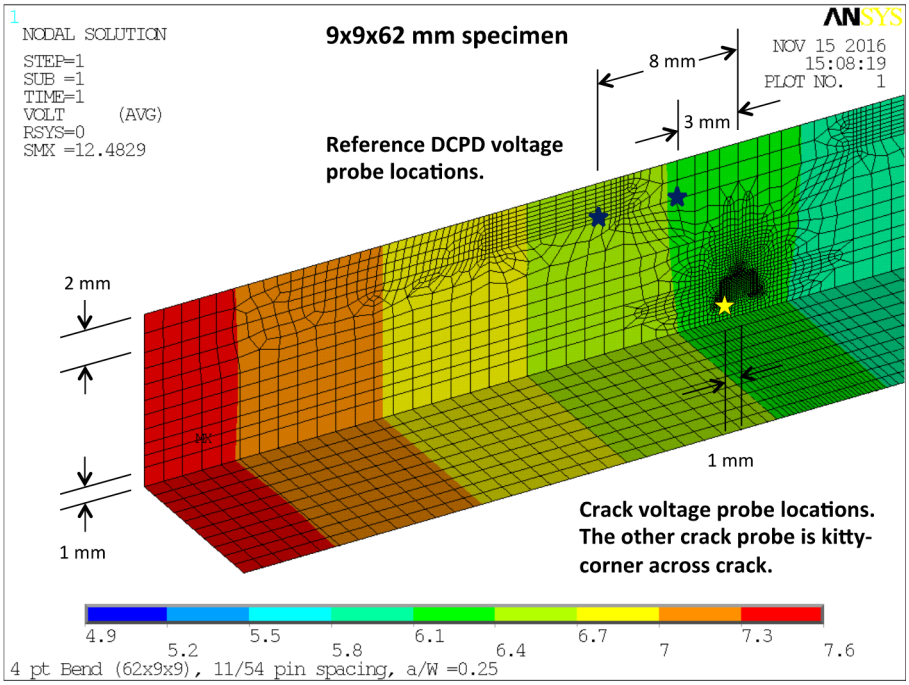

Figure 18. Finite element mesh showing DCPD probe locations for measuring crack voltage and reference resistivity voltage.

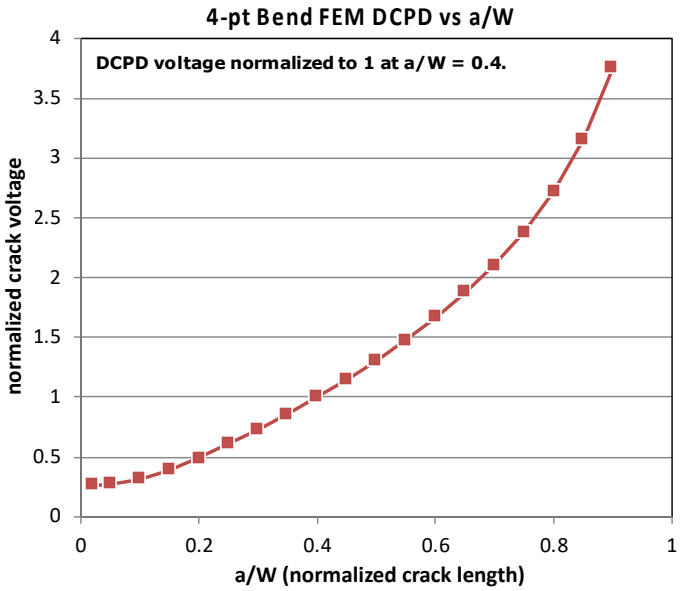

Figure 19. Normalized crack voltage versus normalized crack length as determine from FEM.

5.5 Examples of Usage

An example of an SCCGR test conducted using a notched 4PB specimen in simulated PWR primary water is presented in Figure 20 and Figure 21. This test was run following a typical framework for SCC testing that included gradually less aggressive load cycling steps to allow the fatigue precrack (already present at the start of the test)) to convert to an IGSCC crack, and then this was followed by an observation of constant K SCC crack growth. The decreasing CGR during constant K is not uncommon for Alloy 182, the material used for this test. Post-test observation of crack length was in good agreement with DCPD-estimated crack length. The constant K observation in Figure 21 also shows that DCPD noise levels are ≤2 μm, on par with what PNNL obtains in its CT specimen CGR tests.

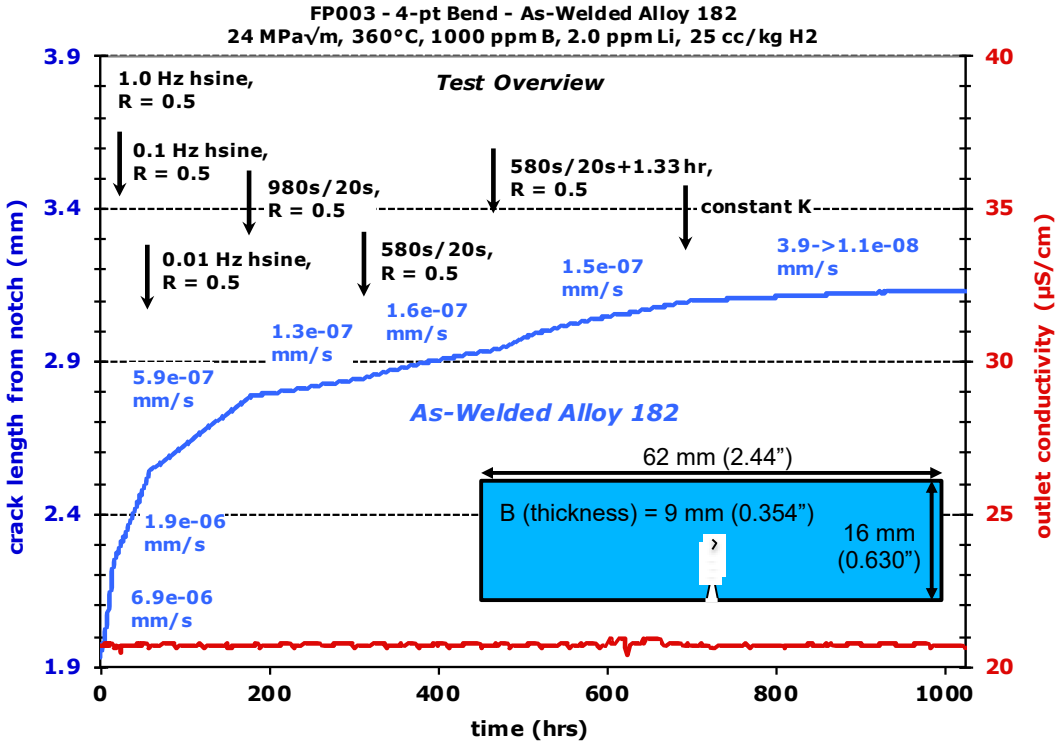

Figure 20. PWSCC crack growth test on an Alloy 182 weld metal specimen conducted using a notched 4PB specimen.

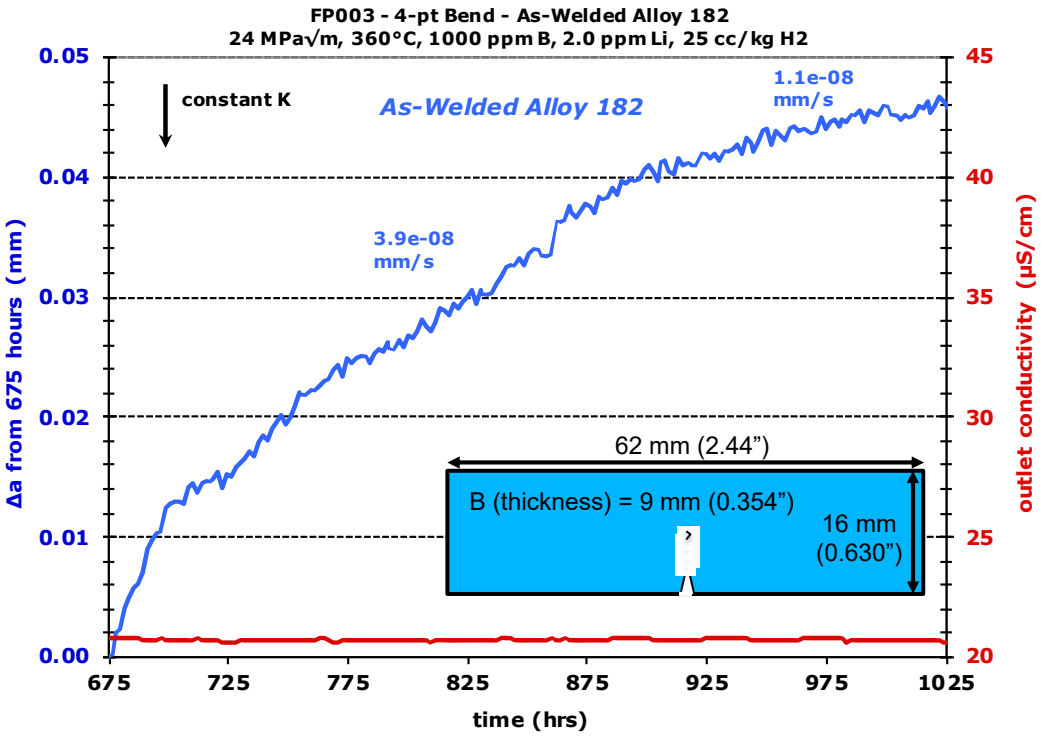

Figure 21. Constant K response during a PWSCC crack growth test on an Alloy 182 weld metal specimen conducted using a notched 4PB specimen. The overall test is presented in Figure 20.

Two shallow crack PWSCC growth tests of an Alloy 182 weld metal in simulated PWR primary water are presented in Figure 22 through Figure 25. Both specimens were produced by first growing an IGSCC crack in a notched 4PB specimen such as in Figure 20. After the crack reached its target length, the test was stopped, and excess material was removed from the specimen to produce an unnotched specimen with a shallow crack. Images of these cracks as they appear on the bottom face of the specimen are shown in Figure 22 and Figure 24. For the first specimen, the crack depth is extremely shallow with no crack present in some locations, while for the second specimen, the crack was clearly deeper and more continuous at the bottom face. After removing excess material and documenting crack morphology and dimensions, constant K PWSCC testing was then resumed at the same stress intensity as for the crack growth test with the notch present. For both specimens, SCC growth readily occurred. The specimen with the shallower crack exhibited a lower SCCGR possibly due to the somewhat lower applied stress intensity or possibly due to the less continuous crack front. In this particular test, extremely low DCPD noise levels of ≤1 µm peak-to-peak were attained. Noise levels such as this are needed to readily measure CGRs below $1x10^{-9}$ mm/s. The second specimen exhibited a fairly high average crack growth rate with the DCPD data showing periodic jumps in crack length. This is sometimes seen in Ni-base alloy weld metals subjected to LWR SCC testing and is thought to be due to uncracked ligaments (typically columnar solidification grains) breaking and thus affecting the DCPD voltage across the crack.

While these demonstration tests are not exhaustive, they clearly show the ability to perform LWR SCCGR tests that obtain in-situ data in the exact same manner as for CT specimen crack growth tests with measured SCCGRs that are typical of the materials being tested. This favorable result along with the desirable specimen shape make 4PB an excellent first choice for quantitative CISCC testing. However, it is recommended that further demonstration tests be performed in an aqueous salt environment to verify desirable performance. Such tests are discussed in the Test Plan section of this report.

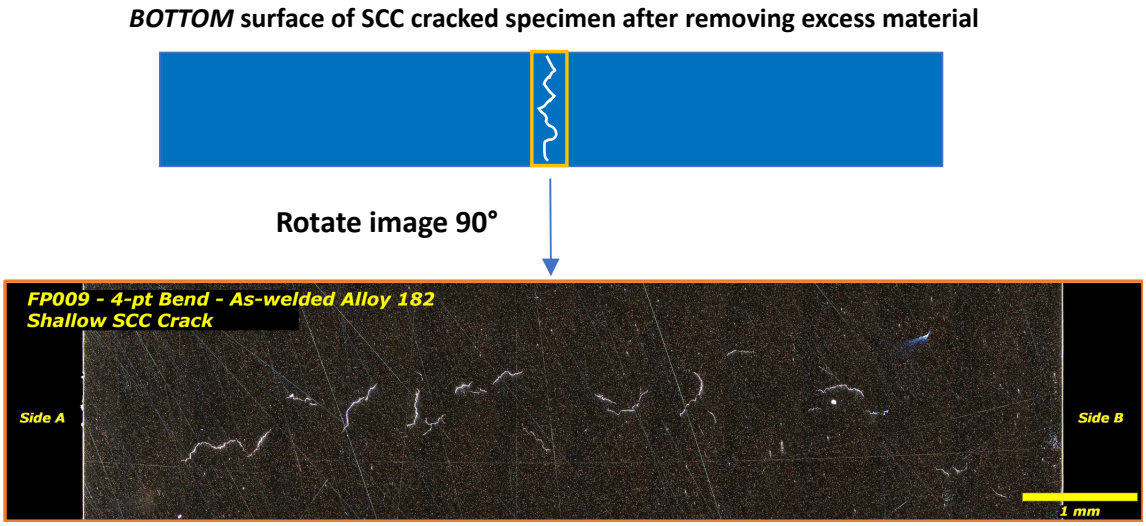

Figure 22. Very shallow (0-0.5 mm deep) SCC crack in a PNNL 4PB specimen as viewed on the tensile loaded bottom surface.

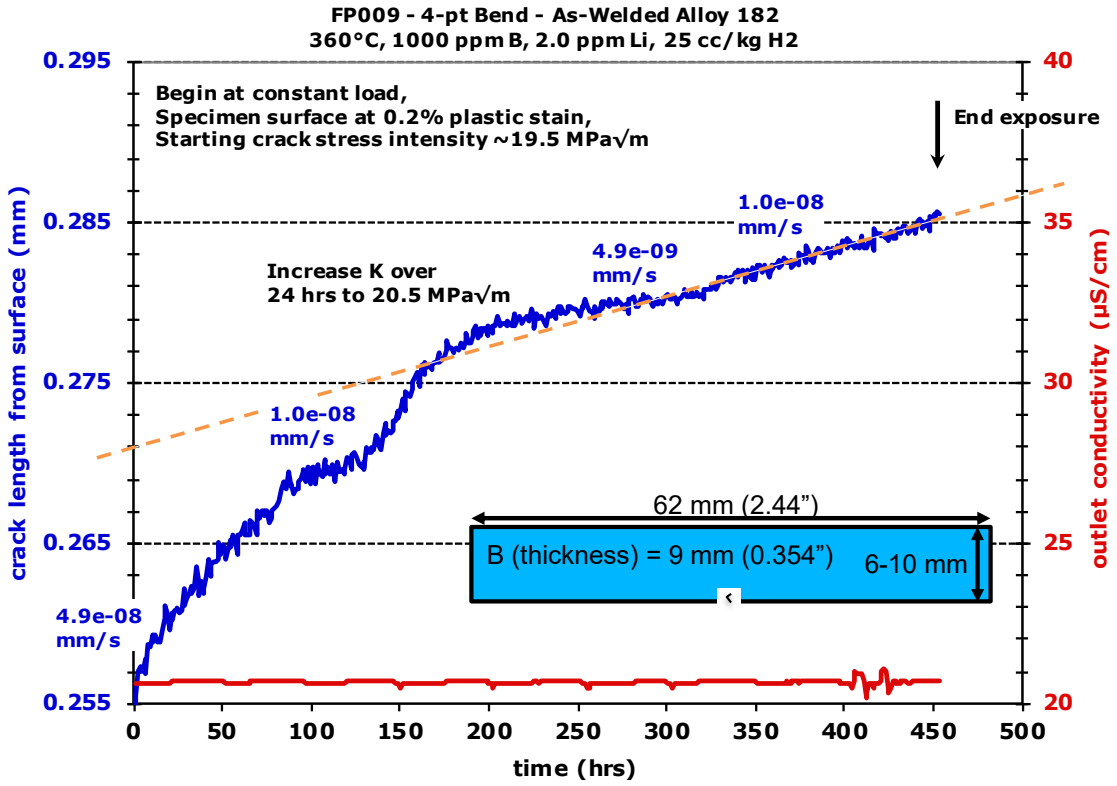

Figure 23. PWSCC crack growth response of a shallow (0-0.5 mm deep) crack in an Alloy 182 4PB specimen loaded to ~20 MPa√m. An image of the starting morphology of the crack on the surface of the specimen is provided in Figure 22.

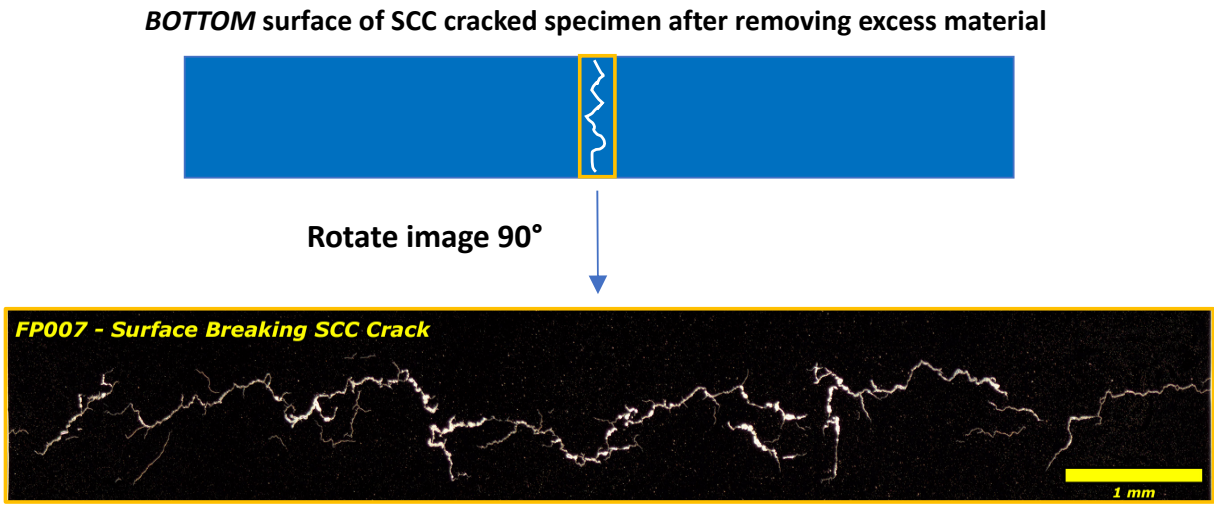

Figure 24. ~0.8 mm deep SCC crack in a PNNL 4PB specimen as viewed on the tensile loaded bottom surface.

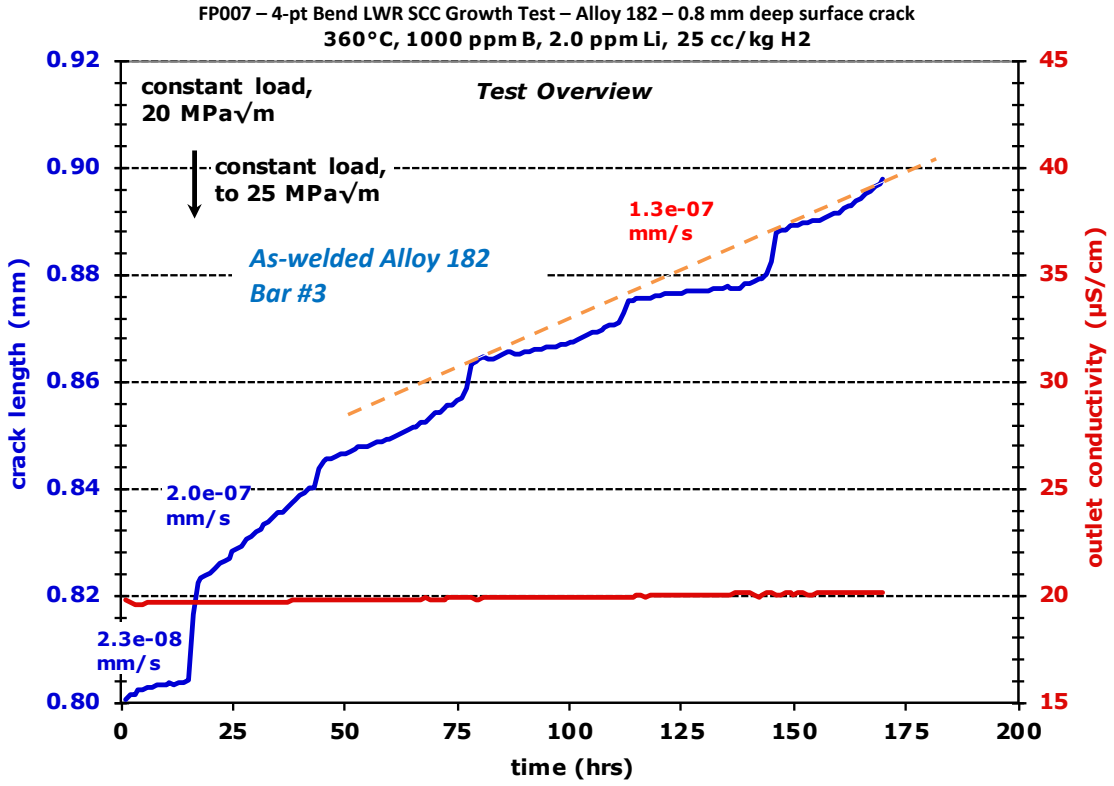

Figure 25. PWSCC crack growth response of a shallow (~0.8 mm deep) crack in an Alloy 182 4PB specimen loaded to ~25 MPa√m. An image of the starting morphology of the crack on the surface of the specimen is provided in Figure 24.

5.6 Test Fixture Development

Extensive efforts have also gone into designing and producing fixtures for conducting 4PB SCC tests. It was paramount that the PNNL 4PB test method have all the same capability as CT specimen tests. This includes the ability to actively load the specimen so that load can be adjusted on-the-fly and also to allow for fatigue cycling to manage the crack front shape, transition to SCC behavior, and advance the crack to sample multiple regions of a specimen. It was also necessary to be able to perform in-situ measurement of crack length by DCPD, so therefore, it had to be possible to electrically insulate the specimen from the fixturing. Key regions of the specimen such as the DCPD probe locations shown in Figure 18 also needed to be accessible. Other desired attributes that were considered as the fixturing was designed are:

- The ability to link multiple fixtures in series in such a way that the load is transmitted to all specimens. The obvious advantage is being able to test multiple specimens in a single environmental chamber. This is important for attaining high throughput.
- The ability to manually apply a preload to a specimen. The primary benefit of this feature is that a small preload is needed to keep a specimen properly aligned in a fixture after its been installed into the fixture.
- If one specimen fails before the others, the test can continue without stopping to remove the specimen.
- The ability to use specimens of different width (W). As already discussed, specimen width can vary from 16 mm to as little as 6 mm depending on the type of test being conducted.
- The ability to adjust the bending (loading) moment applied to a specimen.

A rendering of the fixturing that successfully incorporates all these features is presented in Figure 26. This shows a two-unit assembly. The fixture is comprised of multiple pieces that include load pads, ceramic insulators, an “inner traveler”, a spacer shim, a load transfer pin, and the preload screw. For CISCC testing, the preload screw only serves to keep a specimen and load pads from falling out of a fixture. It does not add to the load on the specimen during a test. This is because the preload screw applies its load independent of the load applied by the servo and since its elastically almost perfectly stiff, so as soon as the servo load exceeds whatever load was applied by the preload screw, the specimen deflects away from the loading bolt. Load is applied to the specimen via the inner traveler and load transfer pin. The inner traveler moves within the fixture and has an available travel of ~2 mm. This is more than sufficient movement to accommodate the specimen deflection needed to load specimens for crack growth rate testing to very high stress intensity or for crack initiation testing to their yield strength or several percent applied plastic strain. Spacer shims of different thickness are used to allow specimens with different W values. Load is serially applied by hanging each specimen off a load transfer pin that goes through the inner traveler. If a specimen cracks excessively, it will deflect to the point where the load transfer pin bottoms out in the hole in the fixture through which the pin passes. When this happens, load is relieved from the specimen, and the fixture itself carries the load. From a mechanical perspective, there is no issue if the specimen fractures, but fracture is nonetheless undesirable because this would sever the DCPD current circuit that runs serially through each specimen, rendering DCPD inoperable.

Examples of actual fixtures with test specimens are presented in Figure 27. The image on the left shows a PNNL 4PB fixture with a crack growth rate specimen while the middle image shows a fixture with a crack initiation or shallow crack growth specimen. As already shown, a variety of LWR SCC tests have been conducted using this fixturing. A simple proof test of nine specimens in a single string such as shown in the rendering on the right side of Figure 27 has also been conducted. While this test method and fixturing were developed for a completely different programmatic need, it has virtually all the features needed to perform high precision, quantitative CISCC growth rate and initiation testing in support of NRC needs.

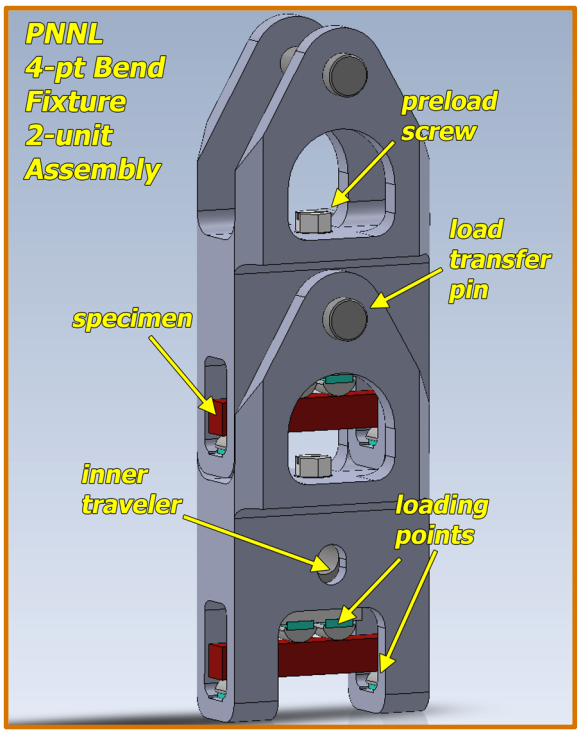

Figure 26. Rendering of a two-unit fixture assembly showing key features.

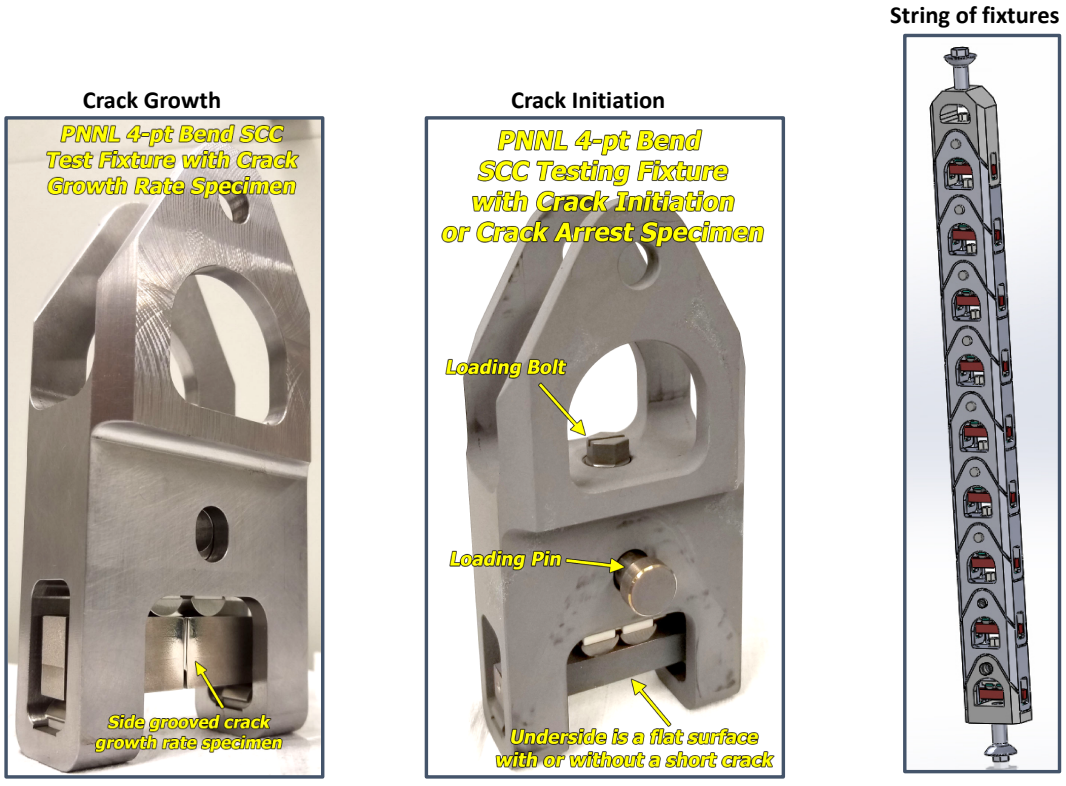

Figure 27. Two images of actual fixtures and a rendering of a string of nine specimens.

6.0 Test Plan

A general overview of a test plan is provided here. Testing is divided into three phases, and the estimated length of time to complete various phases of the test program is based on having two 6-specimen test systems. Additional test systems will reduce the total durations and/or allow for more flexibility in altering the test plan without drastically impacting the schedule.

Phase 1: Calibration of DCPD-estimated crack length in saturated salt solutions. Since this crack length measurement method relies on measuring a resistance, the use of brine solutions that have a 10^4 higher conductivity than simulated PWR primary water may affect the DCPD calibration because the brine solution in the crack can act as a conducting medium. The initial series of tests will aim to establish the use of CT specimens and 4PB specimens for CISCC testing in brine solutions and fine tune the DCPD calibration as needed. A DCPD calibration will first be performed with compact tension specimens. These will be utilized first because their calibration in simulated LWR core cooling water is well known, and any change in calibration in high conductivity brine solutions will be more readily identified. 4PB DCPD calibration will follow and be compared to the CT specimen calibration.

Phase 2: Establish CISCC growth response in brine solutions. Testing in an aqueous solution has the advantage of providing a consistent, known bulk water chemistry. While the crack tip chemistry is expected to differ from the bulk solution chemistry, aqueous testing will provide a much stronger, more consistent link between bulk solution chemistry and the crack tip chemistry than testing salt loaded specimens in humid air. The more consistent and better-known crack tip chemistry will allow for a clearer identification of CISCC response in varying environmental conditions such as stress intensity, temperature, salt concentration, salt composition (including inhibitors), and material condition. A saturated brine environment also represents the best possible migration of a deliquescent solution into a crack during a humid air test where salt has been applied to the surface of a precracked specimen. For this reason, it is thought that SCCGRs observed in humid air tests will be unlikely to exceed those observed during aqueous tests for the same intended salt concentration in the crack. However, at a minimum these tests in water will provide a guide for what could be seen during deliquescent humid air tests. Phase 1 and Phase 2 will overlap somewhat in that some of the data obtained as part of the DCPD calibration are expected to be applicable toward Phase 2 testing. Phase 1 and Phase 2 combined are expected to require approximately 1.5 years to complete. These results will serve as a baseline for comparison to humid air tests, and thus have high value. During this time, the humid air circulation system, potentially with salt fog capability, will be designed and constructed.

Phase 3: Humid air tests are planned to assess many, if not all of the same dependencies measured in brine solutions. A stronger emphasis on material condition and heat-to-heat variability will be incorporated into this test matrix. Because of potential challenges with deliquescent solutions ineffectively migrating down a crack, test response is expected to be more varied, requiring more tests and/or longer test times to effectively evaluate response. Humid air testing will eventually include assessing diurnal cycles. Total time to complete all currently planned tests is 3-4 years. Testing duration can be decreased substantially with the construction of two additional test systems.

Another important factor to consider in selecting a test matrix is material condition. Deformation, especially cold deformation, has been shown to increase SCC susceptibility during LWR SCC testing of stainless steels, Ni-base alloys, and low alloy steels. One simple mechanism postulated for this is that a cold work-induced strength increase of a material reduces the amount of crack tip blunting, therefore raising the crack tip stress intensity for a given applied load. Such a mechanism could readily translate over to CISCC response. Deformation and/or higher strength can be caused by a variety of events, including improper material processing conditions at the alloy fabricator, bending of the plate to make the

cylindrical casks, material or component handling impacts, and local shrinkage strains in the vicinity of the seam weld heat affected zones. In general, all these events are unavoidable, and as a result, the baseline material for a DCSS CISCC testing program should have some level of cold work but deciding what level can be a challenge. Crack initiation and crack growth in LWR pressure boundary components has almost always been associated with deformation of a material from the same factors described for DCSS containers, and the currently postulated level of maximum possible deformation of pressure boundary structures is approximately 10-12% **[37]**. Thus, many LWR SCC pressure boundary material testing programs have included cold worked material in their assessments.

Bending strains caused by rolling 15 mm thick sheet into an ~2.5 m diameter cylindrical shape to make a DCSS is <1% at the outer surface, but shrinkage strains around welds can easily exceed 10% deformation.

Three possible scenarios can be considered for the deformation level of the baseline condition: 1) No cold work, 2) mild cold work, and 3) high cold work. Because virtually all LWR pressure boundary SCC cracks have been associated with unintended deformation, and because unintended deformation is expected in DCSS containers, the use of *non*-cold worked material for a CISCC test program is unlikely to provide realistic service susceptibility estimates. However, it is difficult to justify a particular level of cold work. As a result of fabrication processes (welding and forming operations), isolated local regions of up to ~20% cold work are possible. However, the majority of the cold deformation is expected to be at a lower level. For this test plan, a tentative decision has been made to follow the LWR SCC community and assume a mild level of 10% CW as the baseline deformation condition. Since typical deformation in the containers is tensile deformation (due to plate forming and weld shrinkage strains), the 10% CW level will be achieved using tensile straining methods.

Another important material factor is the heat affected zone (HAZ) around welds. The primary hallmark of an HAZ is sensitization. A variety of microstructure changes can be induced, and for SCC response, the most important microstructure change is a reduction in chromium content along the grain boundaries. This can result in higher SCC susceptibility because chromium aids in producing a stable passive layer. Thus, it will be important to assess HAZ response as part of the testing program.

Another material factor for the test program is heat-to-heat variability. Drawing again on LWR SCC experience, it has been observed that some materials exhibit higher susceptibility than others **[31, 32, 37]**. Whether or not the microstructural factors that affect the variability can be determined, it is necessary to test multiple heats to quantify this variability as best as possible so that service response can be adequately estimated. An extensive characterization of heat-to-heat SCCGR variability requires testing a large number of heats, likely well beyond what has been expected by the DCSS CISCC measurement community. For SCCGR measurements of next generation Ni-base alloys for PWR pressure boundary materials, PNNL tested more than 10 heats of Alloy 690 **[38]**, and for the EPRI Alloy 690 PWSCC crack growth rate database that was assembled from multiple labs across the world, 22 heats were tested **[37]**. For the PNNL research program, only one heat was tested extensively, but several others were tested semi-extensively, and additional heats were tested at key environmental conditions. The current test plan will perform extensive testing on 2-3 heats. Targeted testing of additional heats within a reasonable timeframe would require building additional test systems.

6.1 General Testing Information

This section contains general information about test type, material parameters, and environments to be studied. An outline of a test matrix will be provided in the following two sections.

- Test type: SCCGR
- Specimen type: For SCCGR testing in humid air environments a flat surface 4PB with in-situ measurement of crack length and actively controlled load will be utilized. Initial testing in water will compare 4PB to CT specimen SCCGR response.
- Baseline material: 10% CW 304L SS.
- Surface condition: As-machined, but not important to SCCGR measurements
- Environmental dependencies to be analyzed in order of importance:
  - Temperature, three temperatures – 25, 40, 60°C. The range may be expanded.
  - Salt composition, including the use of inhibitors, and the possibly the effect of chloride loss via extended exposure without replenishing the salt
  - Salt loading, mg/mm^2
  - Relative humidity
  - Realistic daily temperature and relative humidity (RH) variation
  - Stress intensity
- Materials dependencies:
  - Heat-to-heat variability
  - Effect of sensitization
  - Effect of cold work level
- Multispecimen tests, up to 6 specimens in a test system
  - Two duplicate specimens are often sufficient to establish behavior for a given heat and/or thermomechanical starting condition
  - 6-specimen tests could allow for:
    - Heat-to-heat comparison
    - Sensitized vs non-sensitized microstructure
    - Mild cold work vs no cold work
- Baseline test condition in brine solutions
  - Stress intensity: A stress intensity that is above the threshold stress intensity for SCC – The available literature data have widely conflicting values, so it will need to be experimentally determined.
  - Temperature: Tentatively recommended to be 40°C. The baseline temperature for testing in humid air is expected to be 40°C because of its relevance to expected SCC conditions on containers. The deliquescence relative humidity (DRH) is more easily achieved at lower temperatures, and current estimates are that under atmospheric conditions, no deliquescence will occur until container temperatures drop below 40°C. Tests in water at 40°C allows for comparison to humid air tests.
  - Salt composition: $MgCl_2$. This chloride salt has the lowest DRH.
  - Primary salt concentration: Saturated solution at 20°C
  - Alternate concentration: Ocean (approximately 0.6 molar NaCl)

- Baseline test condition in humid air
  - Stress intensity: As determined from tests in brine solutions
  - Temperature: Tentatively recommended to be 40°C because of its relevance to expected SCC conditions on containers. The DRH is more easily achieved at lower temperatures, and current estimates are that under atmospheric conditions, no deliquescence will occur until container temperatures drop below 40°C.
  - Salt composition: $MgCl_2$. This chloride salt has the lowest DRH.
  - Primary salt concentration: Sufficient to allow full coverage on the surface of a specimen.
  - RH: Slightly above the DRH. Expected to be ~40% RH.

6.2 Currently Planned Tests

Presented here are the currently envisioned tests with short descriptions of their purpose, testing setup, and expected length of time to complete. To obtain an estimate of actual time required to finish a particular subsection of the planned tests, divide the system time by the number of test systems being used. As testing progresses, this outline may change.

6.2.1 Tests in Brine Solutions. 26-33 system months to complete. Number of specimens tested: 30

- Water Test Series #1: CT specimen stress intensity dependence in brine solutions
  - Due to a conflicting data on the threshold stress intensity for SCC growth in 304L SS, scoping tests to determine this value are top priority to establish the baseline test condition.
  - Use baseline temperature of 40°C
  - Evaluate saturated NaCl and saturated $MgCl_2$ solutions because the threshold may be salt composition dependent.
  - One loading - 4 specimens, 2 specimens each of 3 heats, change stress intensity on-the-fly, **3-4 months**
- Water Test Series #2: Refine DCPD calibration as needed in brine solutions.
  - High and low concentration comparison
    - Baseline material condition of 10% CW
    - Baseline stress intensity and temperature
    - Begin with CT specimen tests
    - Duplicate results with 4PB tests
    - Adjust calibration as needed
    - High concentration will be a saturated NaCl solution at 20°C
    - Low concentration is ocean concentration (approximately 0.6 molar NaCl)
    - Salt composition is to be determined
  - First loading – CT specimens, high salt concentration, 2 specimens each of 2 heats, evaluate at long crack length, perhaps driving crack by corrosion fatigue and then observing constant load SCC at long crack length, **2-3 months**
  - Second loading – Notched 4PB specimens, same approach as first loading, **2-3 months**
  - Third and fourth loadings –Evaluate at two lower salt concentrations, only necessary if a large crack length correction is needed for high salt concentration, **6 months total for both loadings**

- Water Test Series #2: Compare 4PB notched, 4PB flat surface, and CT specimen response in brine solutions
  - Test conditions
    - Baseline stress intensity, temperature, and high salt concentration
  - Will have CT and notched 4PB data from Water Test Series #1, only need a single loading of flat surface 4PB
  - One loading – Flat 4PB specimens, 2 specimens each of two heats, evaluate in the same manner as for Water Test Series #1, **2-3 months**
- Water Test Series #3: Temperature dependence in brine solutions
  - Flat 4PB specimens
  - Use baseline stress intensity
  - 25, 40, 60°C – Using salt concentration corresponding to saturation at 20°C.
  - One loading - 6 specimens, 2 specimens each of 3 heats, change temperature on-the-fly, **3-4 months**
- Water Test Series #4: 4PB stress intensity dependence in brine solutions
  - Flat 4PB specimens, duplicate result for CT specimens
  - Use baseline temperature and high salt concentration
  - 5, 8, 11, 14, 17, 20 MPa√m
  - One loading - 6 specimens, 2 specimens each of 3 heats, change stress intensity on-the-fly, **3-4 months**
- Water Test Series #5: Inhibitor effects in brine solutions
  - Flat 4PB specimens
  - Use baseline stress intensity, temperature, and high salt concentration
  - Start with no inhibitor, then at least two inhibitor ratios, details to be determined
  - One loading - 6 specimens, 2 specimens each of 3 heats, change inhibitor ratio on-the-fly, **3-4 months**

6.2.2 Tests in Humid Air. 35-49 system months. Number of specimens tested: 60

- Humid Air Test #1: Temperature dependence
  - Baseline stress intensity
  - Slightly above DRH.
  - 25, 40, 60°C
  - One loading - 6 specimens, 2 specimens each of 3 heats, change conditions on-the-fly, **4-8 months**
- Humid Air Test #2: Salt composition dependence
  - Test conditions
    - Baseline stress intensity and temperature
    - Slightly above DRH
    - 1:2 ratio of inhibitor to Cl by weight, then try higher or lower ratio as needed
  - First loading - 6 specimens, 2 specimens each of 3 heats, 1:2 ratio inhibitor to Cl, **3-4 months**

  - Second loading - 6 specimens, 2 specimens each of 3 heats, higher or lower inhibitor to Cl ratio, **3-4 months**
  - Third loading – 6 specimens, 2 specimen each of 3 heats, inhibitor with $MgCl_2$, **3-4 months**
- Humid Air Test #3: Transition from deliquescence to non-deliquescence
  - Test conditions
    - Baseline stress intensity, temperature, salt composition
  - Start above DRH, establish steady growth, drop below DRH, possibly down to crystallization relative humidity (CRH)
  - One test, 6 specimens, 2 specimens each of 3 heats, **3-4 month test**
- Humid Air Test #4: Effect of sensitization
  - Test conditions
    - Baseline stress intensity, temperature, salt composition
    - Above DRH
    - 10% CW material
  - Sensitize material
  - One loading, 6 specimens, 2 specimens each of 3 heats, may assess temperature dependence, K dependence, DRH->CRH, **3-5 month test**
- Humid Air Test #5: Effect of cold work level
  - Test conditions
    - Baseline stress intensity, temperature, salt composition
    - Above DRH
  - 0 and 20% cold work, will combine with 10% CW data from other tests
  - First loading, 6 specimens, 2 specimens each of 3 heats, 20% cold work condition, may assess temperature dependence, K dependence, DRH->CRH, **3-5 month test**
  - Second loading, 6 specimens, 2 specimens each of 3 heats, 0% cold work condition, may assess temperature dependence, K dependence, DRH->CRH, **5-7 month test**
- Humid Air Test #6: Stress intensity dependence
  - Test conditions
    - Baseline stress intensity, temperature, salt composition
    - Above DRH
  - 5, 8, 11, 14, 17, 20 MPa√m
  - One loading, 6 specimens, 2 specimens each of 3 heats, on-the-fly stress intensity changes, **3-5 month test**
- Humid Air Test #7: Realistic diurnal temperature/RH cycles
  - Test conditions
    - Baseline stress intensity, salt composition
    - Environment characteristic of highly ranked ISFSI site
  - One loading, 6 specimens, 2 specimens each of 3 heats, **3-5 month test**

7.0 Summary

Dry cask storage systems are used to store spent nuclear fuel and are placed outside at nuclear power plants across the United States, including in regions where chloride salts are dispersed in the air. These storage systems consist of a sealed 304/316 SS container placed inside of a ventilated concrete casing. Based on experiences with industries that operate in a variety of atmospheric environments where chloride salts deposit on the surface of stainless steel structures, there is a potential for CISCC to occur on the exterior surfaces of the 304/316 SS containers. The range of environments that the stainless steel container may experience will change with time as the container cools over hundreds of years and is not well known due to a recent start in obtaining surveillance data. Early NRC-funded work covering a variety of salt air environments confirmed the susceptibility of 304/316 SS to CISCC using U-bend specimens under some aggressive deliquescent chloride salt conditions. It is unclear at this time whether those conditions will ever overlap with actual DCSS stainless steel container environments. As part of a continued efforts to evaluate CISCC susceptibility, the NRC has funded PNNL to generate a test plan document that aims to further assess stainless steel CISCC susceptibility using more quantitative techniques and based on current understanding of possible environments.

The water used to cool the core of LWRs can cause SCC in some of the pressure boundary materials exposed to that water, and crack growth rate data are a key metric used by the NRC to regulate the inspection frequency of those portions of the pressure boundary structure. The data for this purpose are obtained using state-of-the-art, laboratory-based techniques based primarily on in-situ crack length measurement methods not yet employed in a large scale in support of CISCC evaluations of dry cask storage systems. A review of CISCC studies relevant to dry cask storage systems revealed that a wide range of methods have been utilized to evaluate the susceptibility of 304/316 SS with only a few studies utilizing quantitative measurement methods similar to that used for LWR pressure boundary SCC studies, and those CISCC studies were limited in scope. The remaining CISCC studies are roughly divided between “crack/no crack” assessments and average crack growth rate assessments, both of which use post-test observations of cracks with such observations having reduced regulatory value. For the studies where crack growth rate data have been obtained, a wide variety of specimen types have been employed, often with little regard to how the specimen geometry might affect the evolution of crack tip stresses that can strongly influence CISCC behavior. Besides frequent usage of rudimentary SCC test methods, CISCC measurements have been performed in a wide range of environments, and these two key factors have resulted in a large amount of scatter in the available data.

This test plan document recommends the use of a 4-point bend specimen and fixture system designed for obtaining in-situ crack growth rate data. A 4-point bend geometry is well suited to humid air CISCC testing because the flat surface is amenable to controlled, quantifiable salt deposition techniques onto surfaces with short cracks which is relevant to the expected DCSS CISCC cracking geometry. The specimen dimensions and fixturing allow for multiple specimens to be tested simultaneously in a single test system. In-situ measurement of crack growth rate is attained using a direct current potential drop technique like what is used for LWR core cooling water SCC studies. Development of this 4-point bend capability for LWR SCC testing was recently completed and can readily be adapted to CISCC testing. A portion of the test plan is dedicated to confirming and calibrating this technique to CISCC evaluations.

In the last several years, there has been a better understanding of when deliquescent conditions needed for CISCC are likely to occur on the stainless steel containers. The recommended test matrix takes this into account. A review of the CISCC literature revealed a lack of assessment of material conditions that may affect CISCC susceptibility such as HAZ evaluation and material strength level. There is also a lack of assessment of heat-to-heat variability, and the test matrix incorporates all these aspects. The recommended test plan would require 4-6 years to complete.

8.0 References

1. X. He, T.S. Mintz, R. Pabalan, L. Miller, G. Oberson, “Assessment of Stress Corrosion Cracking Susceptibility for Austenitic Stainless Steels Exposed to Atmospheric Chloride and Non-Chloride Salts”, NUREG/CR-7170, U.S. Nuclear Regulatory Commission, February 2014 (ADAMS Accession No. ML14051A417).
2. P. Ramuhalli, P.G. Heasler, T.L. Moran, A.E. Holmes, M.T. Anderson, “Reliability Assessment of Remote Visual Examination,” NUREG/CR-7246 (PNNL-27003), U.S. Nuclear Regulatory Commission, August 2018, (ADAMS Accession No. ML18228A516).
3. Ekstrom P and J Wåle. 1995. Crack Characterization for In-service Inspection Planning. SKI Report 95:70, Swedish Nuclear Power Inspectorate, Stockholm, Sweden.
4. Wåle J. 2006. Crack Characterisation for In-service Inspection Planning - An Update. SKI Report 2006:24, Swedish Nuclear Power Inspectorate, Stockholm, Sweden.
5. S. M. Bruemmer and M. B. Toloczko, “Pacific Northwest National Laboratory Investigation of Stress Corrosion Cracking in Nickel-Base Alloys”, NUREG/CR-7103, Volume 1, U.S. Nuclear Regulatory Commission, Office of Nuclear Regulatory Research, May 2011.
6. M.B. Toloczko, M.J. Olszta, Z. Zhai, S.M. Bruemmer, “Stress Corrosion Crack Initiation Measurements of Alloy 600 in PWR Primary Water”, Proceedings of the 17th International Conference on Environmental Degradation of Materials in Nuclear Power Systems – Water Reactors, August 9-12, 2015.
7. M.B. Toloczko, “Materials Reliability Program: Stress Corrosion Crack (SCC) Initiation Testing of Ni-Base Alloys for PWR Applications – Part 1 (MRP-426)”, Electric Power Research Institute (EPRI), Document #3002010761, 2017.
8. S. LeHong, C. Amzallag, A. Gelpi, "Modeling of Stress Corrosion Crack Initiation on Alloy 600 in Primary Water of PWRs," *Proc. 9th International Symposium on Environmental Degradation of Materials in Nuclear Power Systems - Water Reactors,* The Minerals, Metals, and Materials Society, 1999, pg. 115.
9. Z. Zhai, M. J. Olszta, M. B. Toloczko, S. M. Bruemmer, "Precursor Corrosion Damage and Stress Corrosion Crack Initiation in Alloy 600 During Exposure to PWR Primary Water", *Proc. 17th Int. Conf. Environmental Degradation of Materials in Nuclear Power Systems - Water Reactors,* TMS, 2015.
10. O.E. Albores-Silva, E.A. Charles, C. Padovini, “Effect of Chloride Deposition on Stress Corrosion Cracking of 316L Stainless Steel Used for Intermediate Level Radioactive Waste Containers”, Corrosion Engineering, Science and Technology, 46, 2011, pp. 124-128.
11. T. Prosek, A. Iversen, C. Taxén, D. Thierry, “Low-Temperature Stress Corrosion Cracking of Stainless Steels in the Atmosphere in the Presence of Chloride Deposits”, Corrosion, 65, 2009, pp. 105-117.
12. N.D. Fairweather, N. Platts, D.R. Tice, “Stress-Corrosion Crack Initiation of Type 304 Stainless Steel in Atmospheric Environments Containing Chloride: Influence of Surface Condition, Relative Humidity, Temperature, and Thermal Sensitization”, NACE Corrosion Proceedings, 2008, Paper No. 08485.
13. S. Shoji, N. Ohnaka, “Effects of Relative Humidity and Kinds of Chlorides on Atmospheric Stress Corrosion Cracking of Stainless Steels at Room Temperature”, Boshuku Gijutsu, 38, 1989, pp. 92-97.
14. A. Kosaki, “Evaluation Method of Corrosion Lifetime on Conventional Stainless Steel Canister under Oceanic Air Environment”, Nuclear Eng and Design, 238, 2008, pp. 1233-1240.

15. A.J. Duncan, P.-S. Lam, R.L. Sindelar, Joe T. Carter, “Crack Growth Rate Testing with Instrumented Bolt-Load Compact Tension Specimens under Chloride-Induced Stress Corrosion Cracking Conditions in Spent Nuclear Fuel Canisters”, NACE PVP Proceedings, 2017, Paper No. 66105.
16. H. Hayashibara, M. Mayuzumi, Y. Mizutani, J. Tani, “Effects of Temperature and Humidity on Atmospheric Stress Corrosion Cracking of 304 Stainless Steel”, NACE Corrosion Proceedings, 2008, Paper No. 08492.
17. M. Speidel, “Stress Corrosion Cracking of Stainless Steels in NaCl Solutions”, Met Trans A, 12A, 1981, pp. 779-789.
18. J. Tani, M. Mayzumi, N. Hara, “Stress Corrosion Cracking of Stainless-Steel Canister for Concrete Cask Storage of Spent Fuel”, Journal of Nuclear Materials, 379, 2008, pp. 42.47.
19. K. Shirai, J. Tani, T. Saegusa, “Study on Interim Storage of Spent Nuclear Fuel by Concrete Cask for Practical Use - Feasibility Study on Prevention of Chloride Induced Stress Corrosion Cracking for Type 304L Stainless Steel Canister,” CRIEPI N10035, Central Research Institute of Electric Power Industry, Tokyo, Japan, 2011 (In Japanese).
20. Y. Xie, “Chloride-Induced Stress Corrosion Cracking in Used Nuclear Fuel Welded Stainless Steel Canisters”, Ph. D. Thesis, Ohio State University, 2016.
21. A. Turnbull, S. Zhou, “Impact of Temperature Excursion on Stress Corrosion Cracking of Stainless Steels in Chloride Solution”, Corrosion Science, 50, 2008, pp. 913-917.
22. S. Shoji, N. Ohnaka, Y. Furutani, T. Saito, “Effects of relative Humidity on Atmospheric Stress Corrosion Cracking of Stainless Steels”, Boshuku Gijutsu, 35, 1986, pp. 559-565.
23. L. Miller, T.S. Mintz, X. He, R. Pabalan, Y.-M. Pan, G. Oberson, D. Dunn, “Effect of Stress Level on the Stress Corrosion Cracking Initiation of Type 304L Stainless Steel Exposed to Simulated Sea Salt”, https://www.nrc.gov/docs/ML1322/ML13220A332.pdf, 2013.
24. P.L. Andresen, M. Morra, “Effects of dK/da on SCC Growth Rates”, NACE Corrosion Proceedings, 2007.
25. C.A. Bryan, E.J. Schindelholz, “Properties of Brines formed by Deliquescence of Sea-Salt Aerosols”, Sandia National Laboratory, SAND2017-11231C, 2017.
26. T.S. Mintz, D.S. Dunn, “Atmospheric Chamber Testing to Evaluate Chloride Induced Stress Corrosion Cracking of Type 304, 304L, and 316L Stainless Steel”, NACE Corrosion Proceedings, 2009, Paper No. 09295.
27. C. Bryan, D. Enos, “Summary of Available Data for Estimating Chloride-Induced SCC Crack Growth Rates for 304/316 Stainless Steel, Sandia National Laboratory, SAND2016-299R, 2016.
28. J. Gorman, K. Fuhr, J. Broussard, “Literature Review of Environmental Conditions and Chloride-Induced Stress Degradation Relevant to Stainless Steel Canisters in Dry Cask Storage Systems”, EPRI, Report Number 3002002528, 2014.
29. J.E. Broussard, C. Bryan, R. Sindelar, P.-S. Lam, “Crack Growth Rate Model for CISCC of Stainless Steel Canisters”, NACE PVP Proceedings, Paper No. PVP2019-94055, 2019.
30. J.-I. Tani, M. Mayuzumi, N. Hara, “Initiation and Propagation of Stress Corrosion Cracking of Stainless Steel Canister for Concrete Cask Storage of Spent Nuclear Fuel”, Corrosion, 65, 2009, pp. 187-194.
31. Materials Reliability Program (MRP) Crack Growth Rates for Evaluating Primary Water Stress Corrosion Cracking (PWSCC) of Thick-Wall Alloy 600 Materials (MRP-55) Revision 1. EPRI, Palo Alto, CA: 1006695, 2002.

32. Materials Reliability Program: Crack Growth Rates for Evaluating Primary Water Stress Corrosion Cracking (PWSCC) of Alloy 82, 182, and 132 Welds (MRP-115). EPRI, Palo Alto, CA: 1006696, 2004.
33. xLPR Version 1.0 Report: Technical Basis and Pilot Study Problem Results, U.S. NRC, ML110660292, 2011.
34. D.T. Spencer, M.R. Edwards, M.R. Wenman, C. Tsitsios, G.G. Scatigno, P.R. Chard-Tuckey, "The Initiation and Propagation of Chloride-Induced Transgranular Stress-Corrosion Cracking (TGSCC) of 304L Austenitic Stainless Steel Under Atmospheric Conditions", Corrosion Science, 88, 2014, pp. 76-88.
35. E. A. Richey, D.S. Morton, W.C. Moshier, "Influence of Specimen Size on the SCC Growth Rate of Ni-Alloys Exposed to High Temperature Water", NACE Corrosion Expo 2006, Paper No. 06513.
36. B. Gross and J.E. Srawley, "Stress-Intensity Factors for Single-Edge-Notch Specimens in Bending or Combined Bending and Tension by Boundary Collocation of a Stress Function", NASA Technical Note, NASA TN D-2603, January 1965.
37. Materials Reliability Program: Recommended Factors of Improvement for Evaluating Primary Water Stress Corrosion Cracking (PWSCC) Growth Rates of Thick-Wall Alloy 690 Materials and Alloy 52, 152, and Variants Welds (MRP-386), Electric Power Research Institute (EPRI), Document 3002010756, 2017.
38. M.B. Toloczko, N.R. Overman, M.J. Olszta, and S.M. Bruemmer, "Pacific Northwest National Laboratory Investigation of Stress Corrosion Cracking in Nickel-Base Alloys, Part 3", NUREG/CR-7103, Volume 3, July 2016.

Pacific Northwest
NATIONAL LABORATORY

Proudly Operated by **Battelle** *Since 1965*

U.S. DEPARTMENT OF
ENERGY

902 Battelle Boulevard
P.O. Box 999
Richland, WA 99352
1-888-375-PNNL (7665)

www.pnnl.gov